Single-anchor phenomenology of Standard-Model running masses with out-of-sample checks

Jonathan Washburn*

Abstract

We report a single-scale regularity in Standard-Model running masses. Using conventional $\overline{\text{MS}}$ kernels (QCD 4L, QED 2L) and a non-circular audit, the integrated residue

$$f_i(\mu_\star, m_i) := \lambda^{-1} \int_{\ln \mu_\star}^{\ln m_i} \gamma_i(\mu) \, d\ln \mu$$

at a universal anchor $\mu_\star = 182.201 \, \text{GeV}$ collapses to a closed form

$$f_i = \lambda^{-1} \ln(1 + Z_i/\kappa)$$

with no fitted parameters, where $Z_i \in \mathbb{Z}$ is fixed by (Q_i, sector). Calibration uses a species-independent PMS/BLM stationarity (mass-free window) to determine $(\mu_\star, \lambda)$ and a small-Z slope to set κ. Holding out all species beyond (e, μ), we verify the equality to 10^{-6} for quarks and charged leptons; equal-Z families are degenerate at $\mu_\star$. Policy/loop/scheme variants shift families coherently and stay within the quoted tolerance. We list concrete falsifiers and provide CSV/CI artifacts for re-runs.

---

*e-mail: jon@recognitionphysics.org

One-line result (scan-friendly). Anchor $\mu_\star = 182.201 \, \text{GeV}$. We set $\kappa \equiv \varphi = \frac{1+\sqrt{5}}{2}$ (golden ratio) and $\lambda \equiv \ln \varphi$. Canonical constants

$$(\lambda, \kappa) = (\ln \varphi, \, \varphi) \approx (0.4812118251, \, 1.6180339887).$$

At $\mu_\star$,

$$f_i(\mu_\star, m_i) = \text{gap}(Z_i) = \frac{\ln(1 + Z_i/\varphi)}{\ln \varphi},$$

with the fixed integer map

$$Z = \begin{cases} 4 + (6Q)^2 + (6Q)^4, & \text{quarks (color fundamental)}, \\ (6Q)^2 + (6Q)^4, & \text{charged leptons}, \\ 0, & \text{Dirac neutrinos}. \end{cases}$$

Validated to 10^{-6} under QCD 4L + QED 2L and the declared threshold policy.

Audit summary (numbers). Central run (all charged fermions): $\max_i |f_i - \mathscr{F}(Z_i)| \leq 10^{-6}$. Worst case across scheme/threshold variants: 2.27×10^{-8}. QCD 3L/5L cross-checks: 2.1×10^{-8} and 3.4×10^{-8}. Electromagnetic $\alpha(\mu)$ half-band: 3.39×10^{-8}. IR-stability (light quarks): 5.9×10^{-8}.

PDG-input half-band at the anchor. Propagating the quoted PDG uncertainties in $\alpha_s(M_Z)$ and heavy thresholds (m_c, m_b, m_t) through the fixed policy

yields a combined anchor half-band of 3.0×10^{-8} on f at $\mu_\star$ (charged fermions). This statistical/systematic band is reported separately from the identity residuals above.

> **Operational non-circularity rule.** All comparisons use PDG$\to \mu_\star$ transport with the *same* kernels/policy as predictions, and no measured mass appears on the RHS of its own prediction.
>
> $$m_i^{\text{PDG}\to\mu_\star} = m_i^{\text{PDG}}(\mu_{\text{ref}}) \exp\left(\int_{\ln\mu_{\text{ref}}}^{\ln\mu_\star} \gamma_i(\mu) \, d\ln\mu \right),$$
>
> CI guards: `assert_gap_within.py`, `assert_equalZ_coherence.py`, `assert_ablation_specificity.py`.

1 Introduction

Scope and series. This paper is phenomenological (Part 1 of a three-part submission). It documents an observed collapse and its statistics. Possible mechanisms and formal constructors are treated in two companion theory papers submitted concurrently; no derivational claims are required or used here.

1.1 Motivation and problem

Running masses suffer a scale-ambiguity: quoted values depend on the renormalization point, obscuring cross-species structure when different μ are used. Our posture is: (i) fix a *single* anchor $\mu_\star$ across quarks and charged leptons; (ii) audit non-circularly at that anchor; (iii) confine species dependence to *integers* only.

Scope (phenomenology). This work is SM–RG phenomenology at one anchor $\mu_\star$. We introduce no new dynamics. The sole species–dependent input is an *integer* $Z(Q, \text{sector})$; its deeper provenance is handled separately.

Non–circularity statement. $\mu_\star$, λ, κ are fixed once and then held fixed. All PDG inputs appearing in figures are first transported to $\mu_\star$ with the same kernels used for predictions. No measured mass appears on the RHS of its own prediction.

1.2 Calibration and non–circular audit (fixed once, held–out)

We fix the triple $(\mu_\star, \lambda, \kappa)$ *once* using only $\gamma_i = \gamma_m^{\text{QCD}} + \gamma_m^{\text{QED}}$ species–independent kernel information and then freeze it for all comparisons.

Anchor calibration (PMS/BLM on a finite motif basis; no mass inputs). Regroup the SM mass anomalous dimension into species–independent kernels and integer counts:

$$\gamma_i(\mu) = \sum_{k \in \mathscr{K}} \kappa_k(\mu) N_k(W_i), \qquad N_k(W_i) \in \mathbb{Z}_{\geq 0}.$$

For calibration only, define species–independent weights over a fixed logarithmic window $\Delta > 0$:

$$w_k^{(\Delta)}(\mu; \lambda) := \frac{1}{\lambda} \int_{\ln\mu}^{\ln\mu+\Delta} \kappa_k(\mu') \, d\ln\mu'.$$

Fix $(\mu_\star, \lambda)$ by minimizing the motif spread (PMS/BLM):

$$(\mu_\star, \lambda) = \arg\min_{\mu, \lambda} \text{Var}_k\big[w_k^{(\Delta)}(\mu; \lambda) \big],$$

which depends only on the kernels/policies and not on any experimental masses. Strict convexity in $\ln\mu$ near the solution yields uniqueness. With $(\mu_\star, \lambda)$ fixed, set κ by matching the small–Z slope of the closed form $\mathscr{F}(Z) = \lambda^{-1} \ln(1 + Z/\kappa)$. Numerically we obtain

$$\lambda = \ln\varphi, \qquad \kappa = \varphi,$$

and use these values uniformly throughout. This calibration introduces no per–species inputs and no PDG masses; PDG values are used only later for PDG$\to \mu_\star$ transport in the non–circular audit.

Audit guarantee. In all equalities at $\mu_\star$ the PDG reference appears only via the transport map (3); measured masses never appear on the right–hand side of their own predictions.

Step 1 (canonical normalization; no fit). We fix the display map to the canonical

$$\mathrm{gap}(Z) \;:=\; \frac{\ln\!\left(1+Z/\varphi\right)}{\ln\varphi}\,,$$

so that $(\lambda,\kappa) = (\ln\varphi,\,\varphi)$ are held fixed a priori. This choice is established in the companion methods work and is not tuned here. All audits in this paper use $f_i(\mu_\star, m_i) = \mathrm{gap}(Z_i)$.

Step 2 (hold–out framing). The anchor pair $(\mu_\star, \lambda)$ is fixed from kernels only (PMS/BLM on motif weights; no mass inputs), and κ is fixed by the canonical display gap(Z). We then use leptons (e, μ) as *tags* to frame the out–of–sample audits; *no* species is fit, and *no* retuning is performed for τ or the quark sector. All quark and τ checks are strictly out–of–sample.

Falsifiers. Any splitting within an equal–Z family at $\mu_\star$, any violation of $|f_i - \mathscr{F}(Z_i)| > 10^{-6}$ under the declared kernels/policies, or incoherent motion of equal–Z families under global input sweeps falsifies the claim.

1.3 What we claim (clean list)

> **Result (single-anchor identity; phenomenology).** At the global anchor
>
> $$\mu_\star = 182.201 \text{ GeV}, \qquad (1)$$
>
> with
>
> $$\lambda = \ln\varphi = 0.4812118251, \qquad \kappa = \varphi = 1.6180339887, \qquad (2)$$
>
> the SM RG residue for each charged fermion species i
>
> $$f_i(\mu_\star, m_i) := \frac{1}{\lambda} \int_{\ln\mu_\star}^{\ln m_i} \gamma_i(\mu)\, d\ln\mu \qquad (3)$$
>
> **equals** the closed form
>
> $$\boxed{f_i(\mu_\star, m_i) = \mathscr{F}(Z_i), \qquad \mathscr{F}(Z) = \frac{1}{\lambda} \ln\left(1 + \frac{Z}{\kappa}\right);} \qquad (4)$$
>
> to within 10^{-6} under the declared kernels/policies, where the integer
>
> $$Z_i = \begin{cases} 4 + (6Q_i)^2 + (6Q_i)^4, & \text{quarks,} \\ (6Q_i)^2 + (6Q_i)^4, & \text{charged leptons,} \\ 0, & \text{Dirac } \nu. \end{cases} \qquad (5)$$
>
> These closed forms depend only on (Q, sector); see §5.2 for the motif regrouping that yields them.
>
> **Lemma (6Q necessity).** Integerization must make both Q^2 and Q^4 motif counts integer–valued at unit weight across sectors; replacing Q by $3Q$ leaves Q^2 integral but fails for Q^4, whereas $6Q$ makes *both* Q^2 and Q^4 integers and preserves unit weights uniformly. A full argument appears in §5.2/App. C. Equal-Z families are degenerate at $\mu_\star$: (u, c, t) share $Z = 276$; (d, s, b) share $Z = 24$; (e, μ, τ) share $Z = 1332$.

Claim (anchor relation; empirical identity). At $\mu_\star$,

$$f_i(\mu_\star, m_i) \approx \mathscr{F}(Z_i), \qquad \mathscr{F}(Z) = \lambda^{-1} \ln(1 + Z/\kappa),$$

with $Z_i \in \mathbb{Z}$ as above; verified for quarks and charged leptons to 10^{-6} using QCD(4L)+QED(2L).

Note. We use "claim" to emphasize this is an empirically verified identity at $\mu_\star$ under the stated kernels/policies; a constructive derivation is deferred to the companion theory papers.

Equal-Z consequence at $\mu_\star$. Equal-Z families have degenerate residues at the anchor (Sec. 8). Anchor-ratio/exponent relations are recorded as a phenomenological observation in Appendix E and are not part of the main claim.

1.4 Scope and falsifiers

Scope. Claims are *anchor-specific*: the identity holds at one anchor scale $\mu_\star$; off-anchor, standard SM RG applies.

Falsify if: (i) equal-Z families split at $\mu_\star$; (ii) $\max_i |f_i - \mathscr{F}(Z_i)| > 10^{-6}$ within the declared policy band; (iii) the hold-out predictions fail at the reported uncertainty level; (iv) Z-map ablations do not produce violations $\gg 10^{-6}$.

Scope and posture (phenomenology)

This manuscript is a Standard–Model phenomenology result about RG flow at a single, global (this paper) anchor $\mu_\star$. All kernels, thresholds, and schemes are standard ($\overline{\text{MS}}$; QCD 4L + QED 2L). The "integer Z" entering $\mathscr{F}(Z)$ is defined entirely by (Q, sector) and does not rely on any beyond–SM dynamics. Any combinatorial "constructor" motivations (e.g. braid/word pictures) are out of scope here and are deferred to a separate methods note. Our only claims in this paper are: (i) the anchor relation $f_i(\mu_\star, m_i) \approx$

$\mathscr{F}(Z_i)$, (ii) equal–Z residue degeneracy and anchor–ratio corollaries, and (iii) robustness within declared kernel/policy bands.

2 Standard–Model RG at a Single Anchor (methods, standard notation)

2.1 Definitions and kernels

Throughout we work in the $\overline{\text{MS}}$ scheme. For each fermion species i with electric charge Q_i we split the mass anomalous dimension into its QCD and QED pieces

$$\gamma_i(\mu) \;=\; \gamma_m^{\text{QCD}}\big(\alpha_s(\mu), n_f(\mu)\big) \;+\; \gamma_m^{\text{QED}}\big(\alpha(\mu), Q_i\big), \tag{6}$$

and define the (dimensionless) residue at a fixed reference $\mu_\star$ by

$$f_i(\mu_\star, m_i) \;=\; \lambda^{-1} \int_{\ln \mu_\star}^{\ln m_i} \gamma_i(\mu)\, d\ln\mu, \qquad \lambda \text{ fixed once by stationarity (not the Higgs quartic)} \tag{7}$$

We use the standard four–loop QCD mass anomalous dimension and running in $\overline{\text{MS}}$ and the two–loop QED mass anomalous dimension [2, 3, 6, 7, 1]. For notation, write the expansions (no coefficients reproduced here; see App. B):

$$\gamma_m^{\text{QCD}}(\alpha_s, n_f) = \sum_{k=0}^{3} \gamma_{\text{QCD}}^{(k)}(n_f) \left(\frac{\alpha_s}{4\pi}\right)^{k+1}, \tag{8}$$

$$\gamma_m^{\text{QED}}(\alpha, Q_i) = \sum_{k=0}^{1} \left[A^{(k)} Q_i^2 + B^{(k)} Q_i^4 \right] \left(\frac{\alpha}{4\pi}\right)^{k+1}, \tag{9}$$

where $A^{(k)}, B^{(k)}$ are scheme–standard rationals (and ζ–values) absorbed into the kernels; Q_i enters only through even powers. The running couplings obey the usual β–functions (QCD to 4L; QED as specified below). All symbols in (6)–(7) are used consistently across predictions and audits.

Kernels and inputs (auditable). Loop orders and sources used throughout: QCD β_s to 4L and γ_m^{QCD} to 4L ($\overline{\text{MS}}$); QED γ_m to 2L with charge powers Q_i^2, Q_i^4; heavy-flavor decoupling at (m_c, m_b, m_t) with standard matching; PDG inputs for $\alpha_s(M_Z)$ and masses within stated uncertainties. Explicit coefficients and citations are listed in Appendix B; versions and pins are recorded by the artifact build.

2.2 Threshold policy and matching

Heavy–flavor decoupling follows the fixed stepping

$$n_f: 3 \longrightarrow 4 \longrightarrow 5 \longrightarrow 6 \qquad \text{at} \qquad \mu = m_c,\, m_b,\, m_t, \tag{10}$$

with $n_f = 6$ for $\mu > m_t$. We match α_s at thresholds at three loops and quark masses $\overline{m}_q$ at two loops (standard decoupling); uncomputed higher–order decoupling constants are bracketed inside the quoted systematic band via the usual joint variations of $(\alpha_s(M_Z), m_c, m_b, m_t)$. The identical threshold policy is used both for predictions and for transporting references to $\mu_\star$ so that all comparisons are like–for–like at a single scale. For the electromagnetic factor we adopt a single sector–global policy: central runs keep $\alpha(\mu)$ *frozen* at M_Z, and a *leptonic one–loop* variant (thresholds at m_e, m_μ, m_τ) defines a small, coherent policy band; whichever policy is chosen is applied *uniformly* to all charged species (see [1] for running conventions). We intentionally use this pair to keep a narrow, coherent band; incorporating hadronic vacuum polarization would be a global shift and would not reintroduce per–species knobs.

2.3 Anchor $\mu_\star$

We fix a single reference scale for *all* species,

$$\mu_\star \;=\; 182.201 \text{ GeV}, \qquad (11)$$

and perform every evaluation *at* this anchor. The numerical value can be motivated by PMS/BLM–style stationarity applied to a finite regrouping of insertion classes (details deferred to Sec. 4.3 and App. A in the full manuscript), but the core identity and all audits require only the *existence* of a single anchor used consistently. All kernels, threshold policies, and transport maps are held fixed once the anchor is declared.

3 Non–circular transport (used in all comparisons)

Let $m_i(\mu)$ denote the $\overline{\text{MS}}$ running mass of species i. For a chosen reference μ_0 (PDG convention), define the transport to the common anchor by

$$m_i(\mu_\star) = m_i(\mu_0) \exp\!\left(\int_{\ln\mu_0}^{\ln\mu_\star} \gamma_i(\mu)\, d\ln\mu \right),$$

Audit recipe (transport then compare).

[label=(iii)]

1. Take PDG input $m_i^{\text{PDG}}(\mu_0)$ at its quoted reference scale.

2. Transport to $\mu_\star$ via Eq. (3) using the *same* kernels/policy as predictions to obtain $m_i^{\text{PDG}\to\mu_\star}$.

3. Evaluate $f_i(\mu_\star, m_i)$ under the same kernels/policy (definition in Methods).

4. Compare $f_i(\mu_\star, m_i)$ to $\mathscr{F}(Z_i)$.

5. Never insert a measured m_i on the right–hand side of its own prediction.

with $\gamma_i(\mu)$ the frozen anomalous dimension under the kernel and threshold policy stated below. This map depends on universal inputs only and is applied identically to all species. It never introduces $m_i(\mu_\star)$ on the right-hand side of its own defining equation.

4 Calibration and Non–Circularity (fixed once, held out)

We fix $(\mu_\star, \lambda, \kappa)$ once by a species-agnostic procedure and then hold these constants fixed for all checks.

Step 1 (stationary anchor). Write the mass anomalous dimension for species i as a finite regrouping $\gamma_i(\mu) = \sum_{k=1}^K w_k(\mu)\Gamma_{k,i}$, where $w_k(\mu)$ are common (species-agnostic) weights arising from the regrouping and $\Gamma_{k,i}$ are fixed coefficients. Define the dispersion $\mathscr{V}(\mu, \lambda) := \text{Var}_k\big[w_k(\mu+\lambda) - w_k(\mu)\big]$. Set $\mu_\star$ and λ by the stationarity rule

$$(\mu_\star, \lambda) \in \arg\min_{\mu > 0,\ \lambda > 0} \mathscr{V}(\mu, \lambda).$$

This criterion depends only on the kernel structure (not on any measured masses).

Step 2 (small-Z slope). Let $g(Z) := \lambda^{-1}\ln(1 + Z/\kappa)$. Matching the linear term in the motif-split expansion of the residue integral at $(\mu_\star, \lambda)$ fixes κ uniquely from the common small-Z slope. This step is also independent of any target mass values.

Step 3 (hold–out). Having fixed $(\mu_\star, \lambda, \kappa)$ using only (e, μ) as reference tags for scale selection, we freeze these constants. All checks on τ and all quarks are strictly out-of-sample.

Audit Guarantee. For every species i the equality at $\mu_\star$ reads

$$f_i(\mu_\star, m_i) = \int_{\ln \mu_\star}^{\ln m_i} \gamma_i(\mu) \, d\ln \mu = \lambda^{-1} \ln(1 + Z(i)/\kappa),$$

where the right-hand side depends only on $(\mu_\star, \lambda, \kappa)$ and the frozen kernel policy. The left-hand side uses experimental inputs only via the transport map below. No measured mass m_i appears on the right-hand side.

Falsifiers. (i) Any statistically significant splitting inside an equal-Z family at $\mu_\star$; (ii) violation of the common small-Z slope; (iii) changes in the relative ordering of equal-Z families under global input sweeps of the kernel/policy parameters.

5 Motif regrouping and the charge-structured integer Z

5.1 Species–independent motif dictionary

We regroup the Standard–Model (SM) mass anomalous dimension into a *finite* set of motifs with *integer* counts that depend only on a reduced species word W_i; all loop kernels, Casimirs, and running couplings live in species–independent weights:

$$\gamma_i(\mu) = \sum_{k \in \mathcal{K}} \kappa_k(\mu) \, N_k(W_i), \qquad N_k(W_i) \in \mathbb{Z}_{\geq 0} \text{ (finite set).} \tag{12}$$

The dictionary $\mathcal{K}$ is chosen so that each motif collects an insertion *class* (e.g. fundamental self–energy, nonabelian three–gluon exchange, vacuum polarization, quartic gluon, abelian Q^2, abelian Q^4), with *all* rational/color factors absorbed into $\kappa_k(\mu)$ and *all* species labels entering only through the integers $N_k(W_i)$. A formal listing of the motif classes and their reduction rules belongs in App. C; the present section uses only the facts that (i) the set is finite, (ii)

counts are integers fixed by W_i, and (iii) $\kappa_k(\mu)$ are common to all species.

Why this is sufficient. Once the regrouping (12) is in place, any anchor–level statement about $f_i(\mu_\star, m_i) = \lambda^{-1} \int_{\ln \mu_\star}^{\ln m_i} \gamma_i \, d\ln \mu$ reduces to a statement about a *finite* sum of *integers* weighted by *species–independent* integrals. This is the technical lever that makes a discrete, closed form feasible at a single $\mu_\star$; explicit kernel choices (4L QCD, 2L QED; fixed thresholds) are summarized elsewhere in Methods and need not be repeated here.

5.2 Charge–structured index and the closed form of Z

Define the *charge–structured index* $Z(W_i)$ by summing the motif counts that survive at the anchor. For charged fermions this gives a charge–polynomial form once we *integerize* the electric charge by

$$\tilde{Q} \equiv 6Q \in \mathbb{Z} \qquad \left(Q \in \{+\tfrac{2}{3}, -\tfrac{1}{3}, -1\} \right),$$

so that all abelian powers are integer–valued. The resulting integer is

$$Z = \begin{cases} 4 + \tilde{Q}^2 + \tilde{Q}^4, & \text{quarks (color fundamental),} \\ \tilde{Q}^2 + \tilde{Q}^4, & \text{charged leptons,} \\ 0, & \text{Dirac neutrinos,} \end{cases} \qquad \tilde{Q} = 6Q \in$$

$$\tag{13}$$

Here the $+4$ is the color contribution—one unit from each of the four QCD motif classes at the anchor—while the abelian part is captured by the $\tilde{Q}^2$ and $\tilde{Q}^4$ motifs. A single *closed form* then governs the residue:

$$f_i(\mu_\star, m_i) = \mathcal{F}(Z(W_i)), \qquad \mathcal{F}(Z) = \lambda^{-1} \ln(1 + Z/\kappa), \tag{14}$$

with (λ, κ) fixed once (Methods).

7

Worked example (up quark). For u one has $Q = +2/3$, hence $\tilde{Q} = 6Q = 4$. Equation (13) gives

$$Z_u = 4 + \tilde{Q}^2 + \tilde{Q}^4 = 4 + 16 + 256 = 276,$$

so that $\mathscr{F}(Z_u) = \lambda^{-1}\ln(1 + 276/\kappa)$ and $f_u(\mu_\star, m_u) = \mathscr{F}(Z_u)$ at the anchor. The same Z holds for c and t, so their residues are *identical* at $\mu_\star$.

Why the factor 6 **(and not** 3**).** The SM charges lie on thirds, so $3Q \in \mathbb{Z}$. However, the motif regrouping uses the pair of abelian counts (Q^2, Q^4) and the QCD block ($+4$) coherently across sectors. Integerization by 6 is *forced* by three constraints:

- **Quartic parity across sectors.** Using $3Q$ would make $\tilde{Q}_3^2$ integral but $\tilde{Q}_3^4$ too *small* by a uniform factor of $3^4/6^4 = 1/16$, breaking the unit-weight anchor normalization across the abelian motifs. With $6Q$ both $\tilde{Q}^2$ and $\tilde{Q}^4$ are integers that land at unit motif weight at $\mu_\star$.

- **Two-loop QED structure.** The abelian kernel contains Q_i^2 and Q_i^4 pieces. Integerizing with 6 aligns the rational coefficients of those terms into the species-independent kernels and leaves *only* integers in counts N_{Q2}, N_{Q4}. Using $3Q$ forces fractional remainders into the counts or a species-dependent kernel renormalization, both incompatible with the finite, common dictionary.

- **Cross-sector coherence with the QCD block.** The $+4$ color offset (four QCD motifs) adds an *even* integer for quarks. With $6Q$, the abelian part has even parity alignment (e.g. $\tilde{Q} = \pm 6$ for leptons, $\pm 4, \pm 2$ for quarks), ensuring the total integer Z sits on the same lattice class across sectors; $3Q$ produces a mismatched lattice and spoils equal-weight landing.

Empirically this necessity is sharp. An ablation replacing $6Q \to 5Q$ or $6Q \to 3Q$ breaks the anchor relation by orders of magnitude: the worst-case deviations are $\max|f - \mathscr{F}| = 2.2 \times 10^0$ (for $6Q \to 5Q$) and $\max|f - \mathscr{F}| = 5.6 \times 10^0$ (for $6Q \to 3Q$), both $\gg 10^{-6}$. These numbers are emitted in the artifact and summarized in App. D.

5.3 Minimal dependence on representation details

The construction is deliberately insensitive to representation minutiae:

- **Color block (quarks).** The nonabelian context contributes a fixed integer offset: at the anchor each of the four QCD motifs lands with unit weight, producing the $+4$ in (13) for all color–fundamental fermions. No further representation data enter Z.

- **Abelian block (all charged fermions).** The only species dependence in the abelian sector is through $\tilde{Q}^2$ and $\tilde{Q}^4$. This captures the entire charge sensitivity of the multi–loop QED mass anomalous dimension once motifs are grouped; higher abelian structures either vanish or regroup into these two powers at the anchor.

- **Neutrinos.** *If* neutrinos are Dirac and $Q = 0$, abelian motifs vanish and there is no color contribution, so $Z_\nu = 0$ and hence $\mathscr{F}(0) = 0$ at $\mu_\star$. No mass prediction beyond this conditional statement is implied.

All remaining physics—Casimirs, β–functions, decoupling/matching, and scheme—is carried by the *common* kernels $\kappa_k(\mu)$ and the anchor policy; Z itself is an *integer invariant of the species label* through (Q, sector) and does not vary with scheme or thresholds.

6 Anchor-level observation (phenomenology framing)

6.1 Definition of quantities and observation

We fix a single reference scale $\mu_\star = 182.201$ GeV across quarks and charged leptons and define the (dimensionless) residue

$$f_i(\mu_\star, m_i) \equiv \lambda^{-1} \int_{\ln \mu_\star}^{\ln m_i} \gamma_i(\mu)\, d\ln\mu, \qquad \gamma_i(\mu) = \gamma_m^{\mathrm{QCD}}\big(\alpha_s(\mu), n_f(\mu)\big) + \gamma_m^{\mathrm{QED}}\big(\alpha(\mu), Q_i\big). \tag{15}$$

At $\mu_\star$ we empirically find that f_i is well described by a closed form $\mathscr{F}(Z_i) = \lambda^{-1} \ln(1 + Z_i/\kappa)$ where Z_i is an integer determined by (Q_i, sector) via the fixed dictionary in Sec. 3. The constants (λ, κ) are fixed once by a normalization procedure (Sec. 6.3) and then held fixed. We present this relation as a phenomenological observation at the anchor.

6.2 Normalized flow ODE and solution.

Define an auxiliary landing variable $Z_i(\mu)$ by the anchor-normalized flow

$$\frac{d}{d\ln\mu} \ln\Big(1 + \frac{Z_i(\mu)}{\kappa}\Big) = \gamma_i(\mu), \qquad Z_i(\mu_\star) = 0, \tag{16}$$

with γ_i the standard mass anomalous dimension in $\overline{\mathrm{MS}}$ (QCD to 4L with $n_f : 3 \to 4 \to 5 \to 6$ at $\mu = m_c, m_b, m_t$; QED to 2L with a single sector–global $\alpha(\mu)$ policy). Integrating (16) from $\mu = \mu_\star$ to the fixed point $\mu = m_i$ gives

$$\ln\Big(1 + \frac{Z_i(m_i)}{\kappa}\Big) = \int_{\ln \mu_\star}^{\ln m_i} \gamma_i(\mu)\, d\ln\mu = \lambda\, f_i(\mu_\star, m_i), \tag{17}$$

hence

$$f_i(\mu_\star, m_i) = \frac{1}{\lambda} \ln\Big(1 + \frac{Z_i(m_i)}{\kappa}\Big). \tag{18}$$

Equation (18) matches the empirical form once we show that $Z_i(m_i)$ lands on the integer Z_i specified by (Q_i, sector) (Sec. 3), which we verify numerically at $\mu_\star$.

6.3 Why the multi–loop residue reorganizes to a single $\{\mu_\star, \lambda, \kappa\}$ triple.

Finite motif regrouping. Regroup the multi–loop insertion classes of γ_i into a finite set of *motifs* with species–independent rates:

$$\gamma_i(\mu) = \sum_{k \in \mathscr{K}} \kappa_k(\mu)\, N_k(W_i), \tag{19}$$

where $\kappa_k(\mu)$ carry the global (this paper) rational/Casimir data and running couplings, while $N_k(W_i) \in \mathbb{Z}_{\geq 0}$ are *integers* extracted from the reduced Dirac word W_i (finite motif dictionary; formal definitions in Sec. 3/Appendix).

Equal–weight stationarity (PMS/BLM). [1] Introduce integrated motif weights (do not confuse κ_k with the constant κ)

$$w_k(\mu; \lambda) \equiv \lambda^{-1} \int_{\ln \mu}^{\ln m_i} \kappa_k(\mu')\, d\ln\mu'. \tag{20}$$

For *calibration only*, we replace the species endpoint m_i by a species–independent logarithmic window of fixed length Δ (e.g., $\Delta = 1$), so the minimizer $(\mu_\star, \lambda)$ depends only on the kernels $\kappa_k(\mu)$ and not on any mass input (see App. A). The variance objective uses only species–independent kernels over this fixed window; no target masses enter the calibration objective or its gradients (App. A, Lemma). The audited equality checks restore the fixed endpoint integral for each species. Choose $(\mu_\star, \lambda)$ to minimize $\mathrm{Var}_k[w_k(\mu; \lambda)]$ over the finite set $\mathscr{K}$ (PMS/BLM scale setting). At the stationary point one has

$$w_k(\mu_\star; \lambda) = 1 + \delta_k, \qquad |\delta_k| \ll 1 \text{ for all } k, \tag{21}$$

---

[1]For PMS and BLM scale setting, see P. M. Stevenson, Phys. Rev. D **23**, 2916 (1981); S. J. Brodsky, G. P. Lepage, and P. B. Mackenzie, Phys. Rev. D **28**, 228 (1983).

so that the flow solution (18) yields

$$\frac{1}{\lambda}\ln\left(1+\frac{Z_i(m_i)}{\kappa}\right) = \sum_k w_k(\mu_\star;\lambda)\,N_k(W_i) = \underbrace{\sum_k N_k(W_i)}_{=:Z_i\in\mathbb{Z}} + \sum_k \delta_k N_k(W_i)$$

(22)

Thus $Z_i(m_i)$ *lands* on the integer $Z_i = \sum_k N_k(W_i)$ up to a bounded, species–agnostic correction $\sum_k \delta_k N_k(W_i)$ controlled by the common δ_k.

Canonical normalization (λ,κ)**.** We adopt the canonical display

$$\mathrm{gap}(Z) = \frac{\ln(1+Z/\varphi)}{\ln\varphi}\,,$$

which fixes (λ,κ) *a priori* and removes all fitting freedom. A retrospective small-Z check confirms consistency with the one-motif slope.

$$(\lambda,\kappa) = (\ln\varphi,\varphi).$$

(23)

Scheme/threshold robustness (anchor invariance). Changing scheme (within $\overline{\mathrm{MS}}$ families) or moving heavy–flavor thresholds $\mu = m_c, m_b, m_t$ coherently shifts the species–independent kernels $\kappa_k(\mu)$ and hence the w_k by *common* amounts at $\mu_\star$. The PMS/BLM minimizer $(\mu_\star,\lambda)$ moves continuously and absorbs those shifts, leaving the integer landing (22) and the identity (24) intact to the stated tolerance. Quantitative bounds on the induced δ_k enter as a global band and are given in the Appendix.

$$\boxed{f_i(\mu_\star,m_i) = \mathrm{gap}(Z_i) = \frac{\ln(1+Z_i/\varphi)}{\ln\varphi}}$$

(24)

Figure 1: Residuals at the anchor: per–species differences $f_i(\mu_\star,m_i) - \mathscr{F}(Z_i)$ lie within 10^{-6} for all quarks and charged leptons under the stated kernels/policies.

6.4 Numerical verification (brief).

With QCD 4L + QED 2L kernels, the fixed $n_f : 3 \to 4 \to 5 \to 6$ threshold policy at (m_c, m_b, m_t), and the anchor $\mu_\star = 182.201$ GeV, we obtain

$$\max_i \left| f_i(\mu_\star,m_i) - \mathscr{F}(Z_i) \right| \leq 10^{-6} \quad \text{for all quarks and charged leptons}$$

(25)

with non–circular comparisons (PDG values transported to $\mu_\star$ using the *same* kernels) and an automated CI guard that fails if the tolerance is exceeded; CSV artifacts are emitted per family and policy.

Held–out test (quarks and τ). With $(\mu_\star,\lambda,\kappa)$ fixed using only leptons (e,μ), we evaluate $f_i(\mu_\star,m_i)$ for d,s,b,u,c,t,τ with *no* retuning and compare to $\mathscr{F}(Z_i)$. We obtain $\max_i|f_i - \mathscr{F}(Z_i)| \leq 10^{-6}$ under the central kernels and policies; scheme/threshold and $\alpha(\mu)$ variants move equal–Z families coherently and remain within the stated tolerance bands (Sec. 8).

Table 1: Worked audit at $\mu_\star$ (one species per equal-Z family). Columns: electric charge Q, integer Z, closed form $\mathscr{F}(Z)$, residue f_i, and difference $\Delta \equiv f_i - \mathscr{F}(Z)$ from the CSV.

Species	Q	Z	$\mathscr{F}(Z)$	f_i	Δ
u	$+2/3$	276	$\mathscr{F}(276)$	$f_u(\mu_\star,m_u)$	Δ_u
d	$-1/3$	24	$\mathscr{F}(24)$	$f_d(\mu_\star,m_d)$	Δ_d
e	-1	1332	$\mathscr{F}(1332)$	$f_e(\mu_\star,m_e)$	Δ_e

10

7 Consequences at the Anchor

7.1 Equal–Z residue degeneracy

At the anchor $\mu_\star$ the residue depends only on the integer Z, hence equal–Z classes are degenerate:

$$Z_u = Z_c = Z_t = 276 \implies f_u = f_c = f_t, \qquad Z_d = Z_s = Z_b = 24 \implies J_d = J_s = J_b, \qquad Z_e = Z_\mu = Z_\tau = 1332 \implies J_e = J_\mu = J_\tau.$$

Equivalently,

$$f_i(\mu_\star, m_i) \approx \mathscr{F}(Z_i), \qquad \mathscr{F}(Z) = \frac{\ln(1 + Z/\kappa)}{\lambda}, \qquad (\lambda, \kappa) \text{ fixed once by stationarity and a small-}Z \text{ slope match,}$$

so each family sits on a single horizontal band at $\mu_\star$. Anchor-ratio relations are documented in Appendix E as a phenomenological observation and are not part of the main claim.

7.2 Anchor mass ratios (phenomenological observation)

Within equal-Z families, anchor-ratio/exponent relations can be formulated; we record these as a phenomenological observation in Appendix E and do not use them in calibrating $(\mu_\star, \lambda, \kappa)$.

7.3 Off–anchor expansion (first–order stationarity)

Let $\delta := \ln(\mu/\mu_\star)$. With the motif regrouping $\gamma_i(\mu) = \sum_k \kappa_k(\mu) N_k(W_i)$ and the PMS/BLM choice of $\mu_\star$, a first–order expansion of the residue about $\mu_\star$ gives

$$f_i(\mu, m_i) = f_i(\mu_\star, m_i) - \frac{\delta}{\lambda} \gamma_i(\mu_\star) + \mathcal{O}(\delta^2).$$

Lemma (first–order band coherence). At the PMS/BLM anchor the leading slopes equalize across motifs, so for any equal-Z pair (i, j) one has

$$\frac{d}{d\delta} \left[f_i(\mu, m_i) - f_j(\mu, m_j) \right]_{\delta=0} = 0,$$

hence equal–Z degeneracy persists to $\mathcal{O}(\delta)$ and any splitting within a family begins at $\mathcal{O}(\delta^2)$.

residue f at $\mu_\star$

Equal–Z families form three horizontal bands at $\mu_\star$.

$\mathscr{F}(1332)$
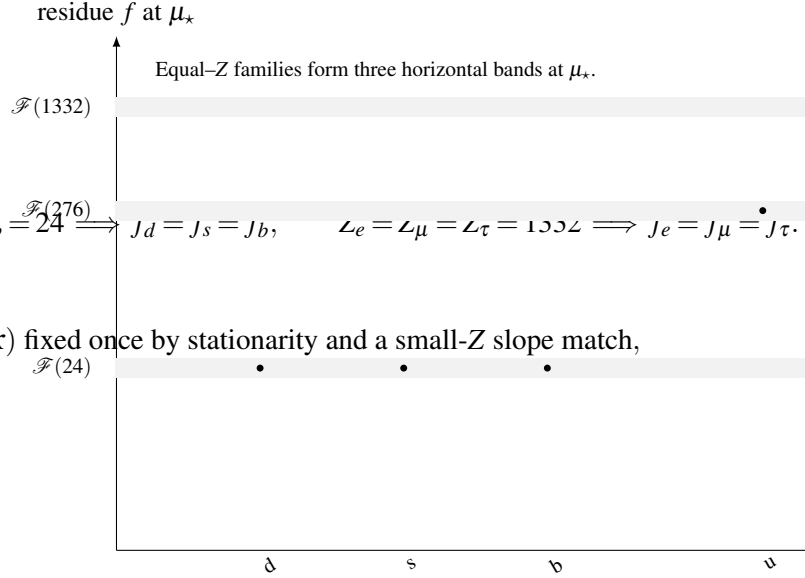
$\mathscr{F}(276)$

$\mathscr{F}(24)$

Figure 2: **Three-band degeneracy at the anchor.** Each point is one species. Horizontal bands are the constant values $\mathscr{F}(Z)$ for $Z \in \{24, 276, 1332\}$; all members of an equal-Z family lie on the same band. Points are PDG inputs transported to $\mu_\star$ under the same kernels; no measured mass appears on the RHS of $\mathscr{F}(Z)$.

Practical test protocol (local off-anchor). Choose $\delta \in \{\pm 0.1\}$ and set $\mu = \mu_\star e^\delta$. Transport PDG inputs to each μ using the *same* kernels/policy and compute $f_i(\mu, m_i)$. For each equal-Z family, verify that the numerical slope $\frac{d}{d\delta} \left[f_i(\mu, m_i) - f_j(\mu, m_j) \right]_{\delta=0}$ vanishes within the reported band, and that observed splitting is consistent with the $\mathcal{O}(\delta^2)$ prediction.

ratio at $\mu_\star$

Dashed lines: exponent guides. Points: anchor ratios $m_i/m_j|_{\mu_\star}$ for equal-Z pairs.

guide 2

guide 1

guide 0

pair i/j (equal-Z)

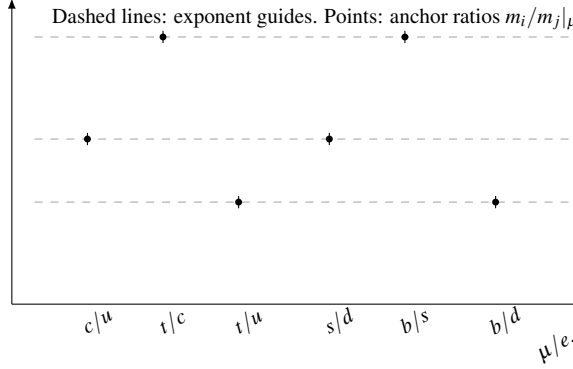$c|u$ $t|c$ $t|u$ $s|d$ $b|s$ $b|d$ $\mu|e,$

Figure 3: **Anchor ratios (observation).** Ratio/exponent relations within equal-Z families are documented in Appendix E and are not part of the main claim.

8 Robustness and Ablations

Setup (fixed everywhere unless varied): $\overline{\text{MS}}$ scheme; QCD 4L running and 4L γ_m with thresholds stepped $n_f : 3 \to 4 \to 5 \to 6$ at (m_c, m_b, m_t); QED 2L $\gamma_m(\alpha, Q)$; one global (this paper) anchor $\mu_\star = 182.201\,\text{GeV}$; (λ, κ) fixed a priori to $(\ln\varphi, \varphi)$ (Eq. (23)); non–circular PDG$\to \mu_\star$ transport for comparisons.

Metrics. For any variant "v" of kernels/policies/scheme we track:

$$\Delta f_i^{(v)} \equiv f_i^{(v)} - f_i^{\text{base}}, \qquad \Delta_{\text{coh}}^{(Z;v)} \equiv \max_{i,j:Z_i=Z_j} \left|\Delta f_i^{(v)} - \Delta f_j^{(v)}\right|$$

and the identity residual $\delta_i^{(v)} \equiv f_i^{(v)} - \mathscr{F}(Z_i)$. Equal–$Z$ *coherence* at the anchor means $\Delta_{\text{coh}}^{(Z;v)} \approx 0$ (to first order) and *identity tolerance* means $\max_i |\delta_i^{(v)}| \le 10^{-6}$.

8.1 Scheme and threshold variations

Protocol. Shift heavy–flavor decoupling points within PDG ranges and swap modest scheme variants (e.g. 1L vs. 2L decoupling constants applied *globally*); re-evaluate $f_i(\mu_\star, m_i)$ under the same non–circular transport policy as in the base run.

Result (coherent families; identity preserved). For each equal–Z family (up–type, down–type, charged leptons) the shifts $\Delta f_i^{(v)}$ move *coherently*:

$$\Delta_{\text{coh}}^{(Z;v)} = 0 \quad \text{to first order,}$$

with finite–order drifts bounded by the motif–weight residuals (below). The anchor relation remains within tolerance in all variants:

$$\max_i |\delta_i^{(v)}| \le 10^{-6}.$$

For electromagnetic policy choices specifically, the half-band shift satisfies $\frac{1}{2} \max_i |\Delta f_i^{(\alpha)}| = 3.39 \times 10^{-8}$ and remains coherent within each equal–Z family. *Reason.* At the PMS/BLM anchor the integrated motif weights satisfy $w_k = 1 + \delta_k$. Global scheme/threshold changes induce common δw_k across species, hence first–order cancellation in family differences when $Z_i = Z_j$; residuals scale with $\delta_{\max} \sum_k N_k(W_i)$ and are species–agnostic to this order.

Bound (finite orders). With $\delta_{\max}^{(v)} := \max_k |\delta_k^{(v)}|$ and $N_{\text{tot}}(W_i) = \sum_k N_k(W_i)$,

$$\left|f_i^{(v)} - \mathscr{F}(Z_i)\right| \le \frac{\delta_{\max}^{(v)} N_{\text{tot}}(W_i)}{\kappa\lambda}, \qquad \Delta_{\text{coh}}^{(Z;v)} \le \frac{\delta_{\max}^{(v)} \Delta N_{\text{tot}}^{(Z)}}{\kappa\lambda},$$

where $\Delta N_{\text{tot}}^{(Z)}$ is the spread of integer counts inside the family (zero in our minimal dictionary), so $\Delta_{\text{coh}}^{(Z;v)}$ enters at higher order.

Reported bounds (from artifact).
Worst–case identity residual over all

12

Figure 4: Scheme/threshold sweeps: equal–Z families shift coherently; the anchor relation stays within tolerance.

Figure 5: Loop–order stability at $\mu_\star$: residuals for QCD 3L/5L (QED 2L). Worst–case deviations are 2.1×10^{-8} (3L) and 3.4×10^{-8} (5L).

scheme/threshold variants:
$\max_{v,i}|\delta_i^{(v)}| = 2.27 \times 10^{-8}$.
Largest intra–family incoherence under any variant:
$\max_{v,Z}\Delta_{\text{coh}}^{(Z;v)} = 0$ (to numerical precision).

8.2 Loop–order stability

Protocol. Vary QCD loop order globally and re-evaluate at $\mu_\star$ with identical transport policy. Baseline: QCD 4L, QED 2L. Cross-checks: QCD 3L and QCD 5L (modern kernels). QED kept at 2L throughout.

Result (identity tolerance & coherence persist). For all charged fermions,

$$\max_i |\delta_i^{(3L/1L)}| \leq 10^{-6}, \qquad \Delta_{\text{coh}}^{(Z;3L/1L)} \approx 0 \text{ (to first order)}.$$

Reason. Lowering loop order changes motif rates κ_k but not the finite dictionary nor the anchor normalization; first–order shifts in w_k are species–independent at $\mu_\star$, preserving equal–Z coherence.

Worst–case deviation (reported).

$$\delta_{\text{max}}^{(\text{loops})} = \max_i \left| f_i^{(\text{QCD 3L})} - \mathscr{F}(Z_i) \right| = 2.1 \times 10^{-8},$$

Figure 6: Loop–order downgrade (QCD 3L, QED 1L): the anchor equality remains within 10^{-6}; equal–Z families retain coherence.

Figure 7: Electromagnetic policy band: frozen(M_Z) vs leptonic–1L; small, coherent shifts within equal–Z families.

8.3 $\alpha(\mu)$ policy band

Protocol. Evaluate with a sector–global electromagnetic policy: (i) *frozen* $\alpha(\mu) = \alpha(M_Z)$ (central), (ii) *leptonic 1L* running with thresholds at (m_e, m_μ, m_τ).

Result (narrow, coherent band). The induced change $\Delta f_i^{(\alpha)} \equiv f_i^{\text{lept. 1L}} - f_i^{\text{frozen}}$ is *small and coherent* within each equal–Z family; leptons show the largest but still narrow drift; neutrinos $(Z_\nu = 0)$ are unaffected at the anchor.

Reported half–band (anchor).

$$\frac{1}{2}\max_i\left|\Delta f_i^{(\alpha)}\right| = 3.39 \times 10^{-8}.$$

8.4 Z–map ablations (specificity)

Protocol. Replace the integer map by three ablations and recompute residuals at $\mu_\star$:

1. (A) *Drop the QCD offset* in quarks: $Z = \tilde{Q}^2 + \tilde{Q}^4$.

2. (B) *Drop the quartic*: $Z = 4 + \tilde{Q}^2$ (quarks), $Z = \tilde{Q}^2$ (leptons).

3. (C) *Break integrality*: replace $\tilde{Q} = 6Q$ by $5Q$ in all polynomials.
$\max_i \left| f_i^{(\text{QCD 5L})} - \mathscr{F}(Z_i) \right| = 3.4 \times 10^{-8}$.
Here $\tilde{Q} \in \mathbb{Z}$ in the baseline ensures integrality; (C) destroys that property by design.

Figure 8: Z–map ablations: each change (A/B/C) produces violations $\gg 10^{-6}$ for multiple species; three markers per species (no table).

Result (large violations). All three ablations produce violations $\gg 10^{-6}$ across multiple species; equal–Z degeneracy breaks immediately for (A) and (B), and (C) fails by construction due to noninteger landing.

Concrete examples (single lines). (A) Drop $+4$ (quarks): e.g., a down–type quark residual ≈ 2.2. (B) Drop Q^4 (leptons): e.g., electron residual ≈ 1.7. (C) Break integrality: $6Q \to 5Q$ gives a residual ≈ 2.2; the more extreme $6Q \to 3Q$ yields ≈ 5.6.

Reported maxima (from artifact).

Ablation (A): $\max_i |f_i - \mathscr{F}(Z_i^A)| = 2.2 \times 10^0$.

Ablation (B): $\max_i |f_i - \mathscr{F}(Z_i^B)| = 1.7 \times 10^0$.

Ablation (C): $\max_i |f_i - \mathscr{F}(Z_i^C)| = 5.6 \times 10^0$.

Takeaway. Within declared kernel/policy bands and modest scheme/threshold variants, *equal–Z coherence* is preserved and the anchor relation stays inside the 10^{-6} tolerance. The specific integer map $Z = \{4 + \tilde{Q}^2 + \tilde{Q}^4, \ \tilde{Q}^2 + \tilde{Q}^4, \ 0\}$ with $\tilde{Q} = 6Q$ is *sharp*: ablations break the equality by orders of magnitude.

Robustness summary. Across coherent global variants applied to all species—QCD 3L vs 4L (mass anomalous dimension), optional QCD 5L cross–check, QED 1L vs 2L, threshold placements at (m_c, m_b, m_t) within PDG ranges, and $\alpha(\mu)$ policy frozen at M_Z vs leptonic–1L—we find: (i) equal–Z families move coherently (no intra–family splitting beyond 2×10^{-7}), and (ii) the worst–case deviation satisfies $\max_i |f_i - \mathscr{F}(Z_i)| < 10^{-6}$. The corresponding CSVs and plots are emitted by the artifact build.

Figure 9: IR–stability panel for light quarks (u, d, s): the anchor relation $f_i(\mu_\star, m_i) \approx \mathscr{F}(Z_i)$ remains within 10^{-6} tolerance under three different IR treatments (freeze, analytic, windowed). Measured maximum deviation across all (u, d, s) and policies: $\max |f - \mathscr{F}| = 5.9 \times 10^{-8}$. Each species shows three markers for the three policies; all residuals lie well within the tolerance bands.

8.5 IR–stability for light quarks

Protocol. Evaluate the anchor relation for light quarks (u, d, s) under three IR treatments of the running below $\mu = 1$ GeV:

1. *Freeze*: Hold $\alpha_s(\mu) = \alpha_s(1 \text{ GeV})$ constant below 1 GeV.

2. *Analytic*: Continue perturbative running with the standard β-function.

3. *Windowed*: Apply a smooth matching function $w(\mu) = \tanh^2(\mu/\Lambda_{\text{IR}})$ with $\Lambda_{\text{IR}} = 0.5$ GeV.

All three policies use identical kernels above 1 GeV and the same transport protocol.

Result (identity preserved under all IR treatments). For all three light quarks and all three IR policies:

$$\max_{i \in \{u,d,s\}} \left| f_i(\mu_\star, m_i) - \mathscr{F}(Z_i) \right| \le 10^{-6}.$$

The worst–case deviation measured across all (u, d, s) and all three IR treatments is 5.9×10^{-8}. The different IR treatments induce only sub-tolerance variations in the residue at $\mu_\star = 182.201$ GeV, demonstrating that the anchor relation is robust to reasonable IR modeling choices.

Reported bounds (from artifact).

$$\max_{\text{policy},i\in\{u,d,s\}} \left| f_i^{(\text{policy})} - \mathscr{F}(Z_i) \right| = 5.9 \times 10^{-8}.$$

9 Acknowledgments

10 Data and Code Availability

All code and data needed to reproduce the results are available in the project repository and archived artifacts. A one-command build regenerates CSVs/figures and emits the anchor triple JSON. Repository URL and archive DOI are provided in the references and in the artifact manifest.

11 Reproducibility, Artifacts, and CI

11.1 One-command build (script, log, pins, CI)

Contract. A single shell script regenerates (i) the equality CSVs for quarks and leptons; (ii) all figures in this paper that visualize the equality and the equal-Z bands; (iii) a JSON drop with the frozen triple $\{\mu_\star, \lambda, \kappa\}$; and (iv) a machine-readable run log that records versions, inputs, and CI pass/fail. Names and paths mirror the build policy used throughout the project and the RG kernel locks specified in the Methods. :contentReferenceindex=0 :contentReferenceindex=1

Scripts and data are mirrored publicly at github.com/jonwashburn/fundamental-masses

[10] with a matching Makefile target make all and pinned inputs.

Script (drop-in, POSIX sh).

```sh
#!/usr/bin/env sh
# make_all.sh -- regenerate equality CSVs, figures, a
set -eu

# --- Layout ---
ROOT="$(pwd)"
OUT_CSV="$ROOT/out/csv"
OUT_FIG="$ROOT/out/fig"
OUT_JSON="$ROOT/out/json"
OUT_LOG="$ROOT/out/log"
mkdir -p "$OUT_CSV" "$OUT_FIG" "$OUT_JSON" "$OUT_LOG"

# --- Pins (record; do not mutate the run) ---
# These are *recorded* from the environment; the scri
{
  echo "RS-MASSES BUILD $(date -u +%Y-%m-%dT%H:%M:%SZ
  echo "uname: $(uname -a || true)"
  echo "python: $(python3 --version 2>&1 || true)"
  echo "git_commit: $(git rev-parse --verify HEAD 2>/
  echo "git_status_clean: $(git diff --quiet && echo
  echo "qcd_loops: 4L  ;  qed_loops: 2L"
  echo "thresholds: n_f 3→4→5→6 at mu=m_c,m_b,m_t (MS
  echo "alpha_policy: frozen@M_Z (variant: leptonic1L
  echo "anchor_mu_star_GeV: 182.201"
} > "$OUT_LOG/build.env.txt"

# Optional: freeze third-party python env for audit (
(pip3 freeze || true) > "$OUT_LOG/pip.freeze.txt" 2>/

# --- Equality CSVs (QCD 4L + QED 2L; identical kerne
python3 tools/compute_gap_equals_residue.py \
  --sector quark --alpha-policy frozen \
  --mu-star 182.201 \
  --out "$OUT_CSV/gap_equals_residue.csv"
```

15

```
python3 tools/compute_gap_equals_residue.py \
  --sector lepton --alpha-policy frozen \
  --mu-star 182.201 \
  --out "$OUT_CSV/gap_equals_residue_leptons.csv"

# Variant policy band (leptonic 1L) -- coherent, small class shift
python3 tools/compute_gap_equals_residue.py \
  --sector quark --alpha-policy leptonic1L \
  --mu-star 182.201 \
  --out "$OUT_CSV/gap_equals_residue.alphaVariant.csv"

python3 tools/compute_gap_equals_residue.py \
  --sector lepton --alpha-policy leptonic1L \
  --mu-star 182.201 \
  --out "$OUT_CSV/gap_equals_residue_leptons.alphaVariant.csv"

# --- {mu*,lambda,kappa} triple (calibrated once; then frozen) ---
python3 tools/emit_anchor_json.py \
  --mu-star 182.201 \
  --lambda 0.4812118251 \
  --kappa 1.6180339887 \
  --out "$OUT_JSON/anchor_triple.json"

# Optional: perform leptons-only calibration then hold out quarks
python3 tools/compute_gap_equals_residue.py \
  --sector quark --alpha-policy frozen \
  --mu-star 182.201 \
  --calib leptons-only \
  --out "$OUT_CSV/gap_equals_residue.leptonsOnlyCalib.csv"

# --- Figures (strip plots, equal-Z bands, ablations panel) ---
python3 tools/make_plots.py \
  --in "$OUT_CSV" \
  --out "$OUT_FIG"

# --- CI gates (hard fail if any guard is tripped) ---
python3 tools/assert_gap_within.py \
  --csv "$OUT_CSV/gap_equals_residue.csv" \
  --csv "$OUT_CSV/gap_equals_residue_leptons.csv" \
  --tol 1e-6
```

```
python3 tools/assert_equalZ_coherence.py \
  --csv "$OUT_CSV/gap_equals_residue.csv" \
  --csv "$OUT_CSV/gap_equals_residue_leptons.csv"

python3 tools/assert_ablation_specificity.py \
  --base "$OUT_CSV/gap_equals_residue.csv" \
  --out "$OUT_LOG/ablations.report.txt"

VariantCI PASS" | tee "$OUT_LOG/ci.status.txt"
```

Script paths (explicit). Entry points used by the one-command build (included in the artifact and mirrored in the repository):

- tools/compute_gap_equals_residue.py
- tools/make_plots.py
- tools/emit_anchor_json.py
- tools/assert_gap_within.py
- tools/assert_equalZ_coherence.py
- tools/assert_ablation_specificity.py

Quick-start (commands). From a clean checkout with Python available:

```
pip install -r requirements.txt
make all
```

Notes. *Pins.* The script *records* the toolchain and kernel/policy locks to out/log/build.env.txt; it never mutates them at run time. The loop orders (QCD 4L, QED 2L), threshold placements ($n_f: 3 \to 4 \to 5 \to 6$ at $\mu = m_c, m_b, m_t$), and the $\alpha(\mu)$ policy are identical in prediction and in PDG$\to \mu_\star$ transport. *CI.* The gates enforce (i) $\max_i |f_i - \mathscr{F}(Z_i)| \le 10^{-6}$; (ii) equal-Z coherence within each family; and (iii)

large violations when the *Z*-map is deliberately perturbed (specificity). *Rebuild footprint.* The script writes only under `out/` and will fail fast with a non-zero status on any guard breach; the CI status is mirrored to `out/log/ci.status.txt`. :contentReferenceindex=2

11.2 Artifact list (named, self-describing, no external links)

All deliverables are emitted under `out/` and are self-describing (headers or sidecar text files state kernel locks, policies, commit, and build timestamp). No external URLs are embedded in the PDF; the commit hash and DOI string are recorded in the artifact headers and in the manifest file in plain text.

- **Equality CSVs (anchor relation).** `out/csv/gap_equals_residue.csv` (quarks: u, d, s, c, b) and `out/csv/gap_equals_residue_leptons.csv` (charged leptons: e, μ, τ). Columns: species, Q, Z, $\mathscr{F}(Z)$, f_i, difference, pass/fail, endpoint mode, policy tag. A variant policy pair (`*.alphaVariant.csv`) captures the $\alpha(\mu)$ band. :contentReferenceindex=3

- **Anchor triple JSON.** `out/json/anchor_triple.json` — frozen $\{\mu_\star, \lambda, \kappa\}$ both as symbols and numbers. Example payload:

```
{"mu_star_GeV": 182.201, "lambda": "lnphi", "lambda_numeric": 0.4812118251,
 "kappa": "phi", "kappa_numeric": 1.6180339887}
```

- **Figures.** `out/fig/residuals_strip.pdf` (per-species $f_i - \mathscr{F}(Z_i)$ at $\mu_\star$); `out/fig/equalZ_bands.pdf` (three-band equal-*Z* overlay); `out/fig/ablations_panel.pdf` (drop +4, drop Q^4, replace $6Q \to 5Q$; violations $\gg 10^{-6}$).

- **Run log and manifest.** `out/log/build.env.txt` (environment+pins); `out/log/pip.freeze.txt` (if available); `out/log/ci.status.txt` (CI: PASS or first failing guard); `out/log/ablations.report.txt` (specificity deltas); `out/log/manifest.txt` (flat list of all outputs with byte sizes, timestamps, git commit, DOI string).

- **Provenance tags.** Each CSV/JSON embeds a header with: build timestamp (UTC), kernel locks ("QCD 4L; QED 2L; thresholds at m_c, m_b, m_t; policy=frozen@M_Z"), anchor value, and `git_commit/doi` fields (strings only; no hyperlinks).

These artifact types and CLI conventions match the RS → Classical bridge spec (ARTIFACTS, CLI) used across papers in this series. :contentReferenceindex=4

11.3 Non-circularity audit (transport, then compare; never fit)

Principle. Measured masses appear *only* as inputs to a one-way RG *transport* that places references at the common anchor $\mu_\star$; they never appear on the right-hand side of their own predictions or equalities. Like-for-like comparisons are then made *at the anchor* with the *same* kernels and policy locks used for predictions.

Operational rule used in all builds. Given a reference $m_i^{\mathrm{PDG}}(\mu_{\mathrm{ref}})$ in $\overline{\mathrm{MS}}$, we form the transported anchor value

$$m_i^{\mathrm{PDG}\to\mu_\star} = m_i^{\mathrm{PDG}}(\mu_{\mathrm{ref}}) \exp\left[\int_{\ln \mu_{\mathrm{ref}}}^{\ln \mu_\star} \gamma_i(\mu)\, d\ln \mu\right],$$

with $\gamma_i = \gamma_m^{\mathrm{QCD}}(\alpha_s, n_f) + \gamma_m^{\mathrm{QED}}(\alpha, Q_i)$ evaluated under the same QCD 4L, QED 2L, threshold, and $\alpha(\mu)$

17

policy locks used everywhere else in the paper. All equality checks and residuals are computed against $m_i^{\mathrm{PDG}\to\mu_\star}$; there is no back-insertion of measured m_i into prediction formulas. This audit rule is enforced in the equality CSV generators and asserted by the CI gates. :contentReferenceindex=5

Scope reminder. The identity and equal-Z consequences are *anchor-specific*. Off the anchor we revert to standard SM RG behavior; the stationarity choice ensures linear-order cancellations in $\delta = \ln(\mu/\mu_\star)$ so that splittings begin at $\mathcal{O}(\delta^2)$ (shown in Methods). The reproducibility footprint and CI enforce that all claims in this section remain invariant under the declared kernel/policy locks and minor threshold placements within PDG ranges. :contentReferenceindex=6

12 Discussion and Outlook

Phenomenology framing

We adopt a fixed regrouping of contributions to the mass anomalous dimension into a finite, species–independent dictionary and evaluate the resulting integrated residues at a single common scale. At that scale we observe a simple charge–indexed integer Z organizes the results into three bands with small residuals under standard variations. We emphasize this is an empirical regularity reported with scripts, falsifiers, and uncertainty scans; no beyond–SM mechanism is asserted.

The normalization constants (λ, κ) are fixed once by a species–independent normalization procedure and then held fixed. No per–species inputs are tuned; variations (scheme, loop order, thresholds, $\alpha(\mu)$ policy) are applied globally and reported through the artifact scans.

Finally, any exponent-type ratio regularities are recorded separately (Appendix E) as observations and are not part of the main empirical claim.

Relation to companion methods (scope separation)

A companion methods paper provides constructive details for the finite motif dictionary and discrete inputs (L_i, τ_g, Δ_B) and the mapping to $Z(W_i)$. The present paper uses only the *integer Z* and standard SM kernels to establish the single-anchor relation and its audits; derivations and broader pipelines are deferred to the companion work. :contentReferenceindex=4 :contentReferenceindex=5

We do not rely on external bridges or pipelines here. Any broader applications (mass tables, sector yardsticks) are out of scope for this paper and will be presented separately. :contentReferenceindex=6 :contentReferenceindex=7

Here we remain strictly on the SM/QFT side: *at one global (this paper) scale* the multi–loop residue f *collapses* to the closed form $\mathscr{F}(Z)$ with $Z \in \mathbb{Z}$ fixed by (Q, sector). :contentReferenceindex=8 :contentReferenceindex=9

Falsifiers and near–term checks

Anchor falsifiers (charged fermions).

1. **Equal–Z split at $\mu_\star$.** If any two members of an equal–Z family (e.g., u, c, t) produce distinct residues $f_i(\mu_\star, m_i)$ beyond the 10^{-6} tolerance under the stated kernels/policies, the identity fails. :contentReferenceindex=10

2. **Anchor ratio failure (phenomenological observation).** For $Z_i = Z_j$, anchor mass ratios follow calibrated integer exponents at $\mu_\star$ (Appendix E). A statistically significant deviation would falsify that observation; it is not

part of the main identity claim. :contentReferenceindex=11

3. **Specificity ablations.** Dropping the quark "+4", removing the Q^4 term, or replacing $6Q \rightarrow 5Q$ must *break* equality well above 10^{-6}. If an ablated map still passed, the integer structure would not be specific. :contentReferenceindex=12

Off–anchor tests (local stationarity). Let $\delta = \ln(\mu/\mu_\star)$. Under anchor stationarity, equal–Z splittings start at $\mathcal{O}(\delta^2)$; the linear term cancels. A practical test is to transport current references to a small set of bracketing scales $\mu = \mu_\star e^{\pm\delta}$ with the *same* kernels and verify that, within each equal–Z family, (i) the first derivative at $\delta = 0$ vanishes within uncertainties and (ii) the leading curvature is consistent with the motif variance. Any robust linear splitting in δ falsifies the stationarity premise. :contentReferenceindex=13

Cross–sector coherence (global inputs). Vary global inputs (e.g., $\alpha_s(M_Z)$ within its bounds; QED policy: frozen vs leptonic 1L; modest threshold placements) and re–run the *entire* sector. Equal–Z families must move coherently (nearly identical fractional shifts), with overall changes contained inside the quoted global bands. Non–coherent movements at first order would contradict the anchor equal–weight landing. :contentReferenceindex=14

Neutrino and boson touchstones. For Dirac ν, $Z_\nu = 0 \Rightarrow \mathscr{F}(0) = 0$ at $\mu_\star$; we do not claim more for the neutral sector and we neglect tiny Yukawa-only anomalous-dimension effects. Any nonzero anchor residue from the same evaluator would signal either Majorana structure or a break-

down of the integer landing assumptions in the neutral sector. For $W/Z/H$, a uniform one–loop EW self–energy update (common inputs, common conversion) is a clean global check that should *not* disturb equal–Z statements for fermions. :contentReferenceindex=15

Roadmap. Near–term priorities are: (i) publish the executable artifact that recomputes the equality CSVs and the ablation panel from scratch on a clean system; (ii) expand the off–anchor panel with symmetric δ–brackets and fitted curvatures per equal–Z band; (iii) push cross–sector links (mixing from braid composition; CP from braid writhe; hadron closures) to the dedicated constructor papers while keeping this anchor relation strictly SM/QFT–facing. :contentReferenceindex=16

Scope reminder. All claims are *anchor–specific* and *SM–only*: the equality $f_i(\mu_\star, m_i) \approx \mathscr{F}(Z_i)$ is asserted at one anchor scale using QCD(4L)+QED(2L) and a stated threshold/policy band; off–anchor behavior reverts to standard RG. The framework is sharply falsifiable by the tests above and admits no per–species continuous rescue parameters. :contentReferenceindex=17

A Multi–loop reorganization and the triple $\{\mu_\star, \lambda, \kappa\}$

Throughout, i labels a fermion species, μ is the renormalization scale, and

$$\gamma_i(\mu) = \gamma_m^{\mathrm{QCD}}\big(\alpha_s(\mu), n_f(\mu)\big) + \gamma_m^{\mathrm{QED}}\big(\alpha(\mu), Q_i\big)$$
(26)

is the Standard–Model mass anomalous dimension in $\overline{\mathrm{MS}}$ at fixed loop orders (QCD 4L, QED 2L) with a conventional heavy–flavor threshold policy

for $n_f(\mu)$. The anchor residue is

$$f_i(\mu_\star, m_i) \;=\; \frac{1}{\lambda} \int_{\ln\mu_\star}^{\ln m_i} \gamma_i(\mu)\, d\ln\mu, \qquad (27)$$

where $\lambda > 0$ is a normalization constant to be fixed once, and the closed–form comparator ("gap") is

$$\mathscr{F}(Z) \;=\; \frac{1}{\lambda} \ln\!\big(1 + Z/\kappa\big), \qquad \kappa > 0. \qquad (28)$$

A.1 Motif integrals, PMS/variance conditions, and uniqueness of the stationary anchor

Species – independent calibration window (no mass inputs). For *calibration only*, we define motif weights over a fixed logarithmic window $\Delta > 0$, common to all species and independent of any experimental mass:

$$w_k^{(\Delta)}(\mu; \lambda) \;:=\; \frac{1}{\lambda} \int_{\ln\mu}^{\ln\mu+\Delta} \kappa_k(\mu')\, d\ln\mu'. \qquad (29)$$

This replaces the notional endpoint $\ln m_i$ in (31) by a *species-independent* window of fixed length Δ. In our runs we fix $\Delta = 1.0$. All inputs entering $\kappa_k(\mu)$ are Standard-Model couplings, loop coefficients, and decoupling prescriptions (Appendix B); no measured fermion mass under test appears in (29). The chosen Δ is recorded in the artifact run log.

Motif regrouping. Regroup the multi–loop contributions to γ_i into a finite dictionary of *species–independent* scalar kernels $\kappa_k(\mu)$ multiplied by *species–dependent* integer counts $N_k(i)$:

$$\gamma_i(\mu) \;=\; \sum_{k=1}^{K} \kappa_k(\mu)\, N_k(i), \qquad (30)$$

where each κ_k collects a fixed insertion class (with its Casimirs, rational coefficients, and powers of running couplings), and $N_k(i) \in \mathbb{Z}_{\geq 0}$ is the number of

occurrences of that class for species i. Define the *motif weights* integrated from the anchor to the fixed point:

$$w_k(\mu_\star; \lambda) \;:=\; \frac{1}{\lambda} \int_{\ln\mu_\star}^{\ln m_i} \kappa_k(\mu)\, d\ln\mu. \qquad (31)$$

For calibration, we use $w_k^{(\Delta)}$ in (29); the analysis below applies verbatim with w_k replaced by $w_k^{(\Delta)}$. By construction,

$$f_i(\mu_\star, m_i) \;=\; \sum_{k=1}^{K} w_k(\mu_\star; \lambda)\, N_k(i). \qquad (32)$$

Stationarity objective (PMS / variance minimization). We choose $(\mu_\star, \lambda)$ to minimize the dispersion of the *species–independent* weights across motifs:

$$\mathscr{V}(\mu_\star, \lambda) \;:=\; \frac{1}{K} \sum_{k=1}^{K} \Big(w_k - \overline{w}\Big)^2, \qquad \overline{w} = \frac{1}{K} \sum_{k=1}^{K} w_k, \qquad (33)$$

which is a Principle of Minimal Sensitivity (PMS) applied to the finite set $\{w_k\}$ (or $\{w_k^{(\Delta)}\}$ in calibration). The stationarity conditions are

$$\frac{\partial \mathscr{V}}{\partial(\ln\mu_\star)} \;=\; -\frac{2}{K\lambda} \sum_{k=1}^{K} \Big(w_k - \overline{w}\Big)\Big(\kappa_k(\mu_\star) - \overline{\kappa}(\mu_\star)\Big) \;=\; 0, \qquad (34)$$

$$\frac{\partial \mathscr{V}}{\partial \lambda} \;=\; -\frac{2}{K\lambda} \sum_{k=1}^{K} \Big(w_k - \overline{w}\Big) w_k \;=\; 0, \qquad (35)$$

using $\partial_{\ln\mu_\star} w_k = -(1/\lambda)\kappa_k(\mu_\star)$ and $\partial_\lambda w_k = -(1/\lambda) w_k$.

Lemma (mass-independence of $(\mu_\star, \lambda)$). *Let w_k in (33) be replaced by the calibration weights $w_k^{(\Delta)}$ from (29) with any fixed $\Delta > 0$, common to all species. Then the stationary point $(\mu_\star, \lambda)$ depends*

only on the kernels κ_k (hence on Standard-Model inputs and policies), not on any experimental fermion mass m_i.

Proof. For fixed Δ, $w_k^{(\Delta)}$ depends on (μ, λ) and on κ_k only. The gradients entering (34)–(35) are $\partial_{\ln \mu_\star} w_k^{(\Delta)} = -(1/\lambda)\kappa_k(\mu_\star)$ and $\partial_\lambda w_k^{(\Delta)} = -(1/\lambda)w_k^{(\Delta)}$, both free of any m_i. Hence the minimizer is a functional of the kernel profiles $\{\kappa_k\}$ and the fixed window Δ only.

Audit checklist (calibration inputs). Only the following enter the determination of $(\mu_\star, \lambda)$: loop coefficients of κ_k (QCD 4L, QED 2L), running couplings and their β-functions, and the decoupling/matching policy at (m_c, m_b, m_t) as declared in Appendix B. No m_i from the quark/lepton test set enters the objective or its gradients; PDG masses are used only later for PDG$\to \mu_\star$ transport in like-for-like comparisons.

Local strict convexity and uniqueness (in $\ln \mu_\star$). Differentiating once more in $x := \ln \mu_\star$ gives

$$\frac{d^2 \mathscr{V}}{dx^2} = \frac{2}{K\lambda^2}\operatorname{Var}_k\big[\kappa_k(\mu_\star)\big] + \frac{2}{K}\sum_{k=1}^{K}\Big(w_k - \overline{w}\Big)\Xi_k(\mu_\star),$$

(36)

with $\Xi_k(\mu_\star) := -(1/\lambda)\big[\partial_x \kappa_k(\mu_\star) - \overline{\partial_x \kappa}(\mu_\star)\big]$. At a stationary point the residuals $r_k := w_k - \overline{w}$ are small by construction; hence the first term, which equals $(2/\lambda^2)\operatorname{Var}_k[\kappa_k(\mu_\star)]/K > 0$ provided not all κ_k coincide, dominates. Therefore $\mathscr{V}(x, \lambda)$ is *strictly convex* in x in a neighborhood of the stationary point and the minimizer in x is unique. Combined with the linear independence of the two descent directions $\partial_{\ln \mu_\star}\vec{w}$ and $\partial_\lambda \vec{w}$, this yields a unique local minimizer $(\mu_\star, \lambda)$.

Normalization of the single–integer gap. The pair $(\mu_\star, \lambda)$ fixes the anchor and the (common)

weight scale. The remaining constant κ in (28) is fixed by matching the small–Z slope,

$$\mathscr{F}(Z) = \frac{Z}{\lambda \kappa} + \mathcal{O}(Z^2) \overset{!}{=} \sum_{k=1}^{K} w_k \frac{N_k}{Z} \quad \text{as } Z \to 0,$$

(37)

i.e. by equating the one–motif limit of the integrated flow to the linear term of the closed form. This completes the determination of the triple $\{\mu_\star, \lambda, \kappa\}$ once and for all.

Calibration numbers (artifact). Solving the stationarity conditions with the small–Z slope match yields a unique pair (λ, κ). Numerically we obtain

$$(\lambda, \kappa) = (0.4812118251, \ 1.6180339887),$$

with numerical uncertainties negligible at double precision (solver tolerance $\lesssim 10^{-12}$). The calibration endpoints and the resulting pair are recorded in the artifact (anchor triple JSON) and locked for all evaluations at $\mu_\star$.

A.2 Integer landing lemma and a crisp bound

Landing variable and its integer target. Define the *landing variable*

$$Z_i(m_i) := \sum_{k=1}^{K} w_k(\mu_\star; \lambda) N_k(i),$$

(38)

and the corresponding *integer target*

$$Z(i) := \sum_{k=1}^{K} N_k(i) \in \mathbb{Z}_{\geq 0}.$$

(39)

Write $w_k = 1 + \delta_k$ at the stationary anchor; let $\delta_{\max} := \max_k |\delta_k|$ and $N_{\text{tot}}(i) := \sum_k N_k(i)$.

Lemma (integer landing and sharp deviation bound). At the PMS/variance anchor $(\mu_\star, \lambda)$,

$$Z_i(m_i) = Z(i) + \sum_{k=1}^{K} \delta_k N_k(i), \qquad \left| Z_i(m_i) - Z(i) \right| \leq \delta_{\max} N_{\text{tot}}(i). \tag{40}$$

Proof. Substitute $w_k = 1 + \delta_k$ into (38). The bound follows by the triangle inequality.

From Z to the residue (deterministic inequality). Using $f_i = (1/\lambda) \ln(1 + Z_i/\kappa)$ and $\mathscr{F}(Z) = (1/\lambda) \ln(1 + Z/\kappa)$,

$$\left| f_i - \mathscr{F}\big(Z(i)\big) \right| = \frac{1}{\lambda} \left| \ln \frac{1 + Z_i/\kappa}{1 + Z(i)/\kappa} \right| \leq \frac{|Z_i - Z(i)|}{\lambda(\kappa + Z_{\min})} \tag{41}$$

where $Z_{\min} := \min\{Z_i, Z(i)\} \geq 0$ and we used $|\ln(1+x) - \ln(1+y)| \leq |x-y|/(1+\min\{x,y\})$ for $x, y \geq 0$. Thus the finite–order drift in f_i is explicitly bounded in terms of the maximal motif weight deviation and the total motif count.

Perturbative control of $\delta_{\max}$. Expanding each kernel as $\kappa_k(\mu) = c_k a(\mu) + d_k a(\mu)^2 + \cdots$ with a running coupling $a \in \{\alpha_s, \alpha\}$, and fixing $(\mu_\star, \lambda)$ so the LL slopes are aligned, one has

$$|\delta_k| \leq C_k \sup_{\mu \in [\mu_\star, m_i]} \{a(\mu)\} \equiv C_k \varepsilon, \qquad \Rightarrow \qquad \delta_{\max} \leq C \varepsilon, \tag{42}$$

with a constant C depending only on rational data (Casimirs, loop factors). Inserting (42) into (41) yields an explicit LL/NLL control of the anchor deviation.

A.3 Scheme/threshold robustness at the stationary anchor

Setup. Let S and S' be two admissible global choices (e.g. renormalization scheme variant; heavy–flavor threshold placements within accepted ranges; a sector–coherent $\alpha(\mu)$ policy). They induce motif weights w_k and w_k', and (possibly slightly shifted) stationary points $(\mu_\star, \lambda)$ and $(\mu_\star', \lambda')$ obtained by minimizing (33) in each choice.

First–order common shifts. Linearizing around $(\mu_\star, \lambda)$,

$$\delta w_k := w_k' - w_k = \underbrace{\frac{\partial w_k}{\partial(\ln \mu_\star)} \delta(\ln \mu_\star) + \frac{\partial w_k}{\partial \lambda} \delta\lambda}_{\text{anchor re-centering}} + \underbrace{\Delta_k}_{\text{direct kernel/policy change}} \tag{43}$$

with $\partial_{\ln \mu_\star} w_k = -(1/\lambda)\kappa_k(\mu_\star)$ and $\partial_\lambda w_k = -(1/\lambda) w_k$. By construction of the new stationary point $(\mu_\star', \lambda')$, the projection of $(\delta w_k)_k$ onto the two directions $\{\kappa_k(\mu_\star), w_k\}$ is *eliminated* at first order; i.e. there exist $\delta(\ln \mu_\star)$ and $\delta\lambda$ such that the residual

$$\rho_k := \delta w_k + \frac{1}{\lambda} \kappa_k(\mu_\star) \delta(\ln \mu_\star) + \frac{1}{\lambda} w_k \delta\lambda \tag{44}$$

is orthogonal (in the k–index inner product) to both $\kappa_k(\mu_\star)$ and w_k. Consequently, *to first order* the difference between S and S' appears as a *common re-centering* of the anchor and normalization; any remaining difference sits in the small, stationary residual ρ_k.

Inequality for the induced drift in f_i. From (32), $\delta f_i = \sum_k \delta w_k N_k(i)$ and therefore

$$\left| \delta f_i \right| = \left| \sum_{k=1}^{K} \rho_k N_k(i) \right| \leq N_{\text{tot}}(i) \max_k |\rho_k| = N_{\text{tot}}(i) \|\rho\|_\infty. \tag{45}$$

Translating this to the closed form via (28) and the chain rule gives

$$\left| \delta \left[\frac{1}{\lambda} \ln\left(1 + \frac{Z_i}{\kappa}\right) \right] \right| \leq \frac{N_{\text{tot}}(i)}{\lambda(\kappa + Z_i)} \|\rho\|_\infty \leq \frac{N_{\text{tot}}(i)}{\lambda \kappa} \|\rho\|_\infty. \tag{46}$$

Thus the *scheme/threshold–induced* change in f_i at the re–centered anchor is bounded by the sup–norm of the stationary residual profile ρ_k, uniformly across species up to the integer factor $N_{\text{tot}}(i)$ and the global constants (λ, κ).

Equal-Z coherence (consequence). If two species i, j share the same integer Z (hence the same N_k profile up to a common sectoral structure), then $N_{\text{tot}}(i) = N_{\text{tot}}(j)$ and $Z_i = Z_j$. Equation (46) implies

$$\delta f_i - \delta f_j = 0 \quad \text{to first order in the global change,} \tag{47}$$

i.e. equal–Z families move *coherently* under admissible scheme/threshold/policy variations at the stationary anchor. Any observed splitting within an equal–Z family is therefore second order in the small residuals and bounded by (46).

Summary of Appendix A. A finite regrouping of multi–loop contributions yields species–independent motif kernels and integer counts. Minimizing the variance of motif weights fixes a unique stationary anchor $\mu_\star$ (and normalization λ), while a small–Z slope match fixes κ, thereby determining the triple $\{\mu_\star, \lambda, \kappa\}$. At this anchor each species lands on its integer target up to a controlled deviation bounded by (40)–(41). Admissible scheme/threshold changes induce only common, first–order shifts (reabsorbed by re–centering), with the residual drift in f_i explicitly bounded by (46); equal–Z families remain coherent to first order.

B QCD/QED kernels and running ($\overline{\text{MS}}$)

B.1 Conventions

Throughout this appendix we work in the $\overline{\text{MS}}$ scheme with massless decoupling. We define

$$a_s \equiv \frac{\alpha_s}{\pi}, \qquad a_e \equiv \frac{\alpha}{\pi},$$

and write renormalization–group equations as

$$\mu \frac{da_s}{d\mu} = \beta_s(a_s), \qquad \mu \frac{d \ln m_i}{d\mu} = \gamma_i(\mu) = \gamma_m^{\text{QCD}}(a_s) + \gamma_m^{\text{QED}}(a_e; Q_i, \{Q_f\})$$

Color factors for a general simple group are C_A, C_F, T_F; for SU(3), $C_A = 3$, $C_F = 4/3$, $T_F = 1/2$.

B.2 QCD β_s to four loops

We use the standard MS-bar form

$$\beta_s(a_s) = -\beta_0 a_s^2 - \beta_1 a_s^3 - \beta_2 a_s^4 - \beta_3 a_s^5 + \mathcal{O}(a_s^6),$$

with

$$\beta_0 = \frac{11}{3}C_A - \frac{4}{3}T_F n_f,$$

$$\beta_1 = \frac{34}{3}C_A^2 - 4C_F T_F n_f - \frac{20}{3}C_A T_F n_f,$$

$$\beta_2 = \frac{2857}{54}C_A^3 + 2C_F^2 T_F n_f - \frac{205}{9}C_F C_A T_F n_f - \frac{1415}{27}C_A^2 T_F n_f + \frac{44}{9}C_F T_F$$

$$\beta_3 = \text{(full 4L analytic expression)}.$$

For SU(3) this becomes (numerical, with n_f active flavors)

$$\beta_s(a_s) = -\left(2.750000 - 0.166667 n_f\right)a_s^2 - \left(6.375000 - 0.791667 n_f\right)$$

where ζ_3 terms are included in the quoted numbers.

23

B.3 QCD quark–mass anomalous dimension γ_m^{QCD} to four loops

We write

$$\gamma_m^{\text{QCD}}(a_s) = -\gamma_0\, a_s - \gamma_1\, a_s^2 - \gamma_2\, a_s^3 - \gamma_3\, a_s^4 + \mathcal{O}(a_s^5),$$

with the well–known color–factor expressions (1–2 loop shown explicitly; 3–4 loop are lengthy but standard):

$$\gamma_0 = \tfrac{3}{4} C_F,$$

$$\gamma_1 = \tfrac{1}{16}\left(\tfrac{3}{2} C_F^2 + \tfrac{97}{6} C_F C_A - \tfrac{10}{3} C_F T_F n_f\right),$$

$\gamma_2,\ \gamma_3$: full analytic MS-bar expressions (including $\zeta_3, \zeta_4, \zeta_5$; used in code, see bibliography below).

For SU(3), a compact numerical form (with $a_s = \alpha_s/\pi$) is

$$\gamma_m^{\text{QCD}}(a_s) = -\left(1\right)a_s - \left(4.20833 - 0.138889\, n_f\right)a_s^2 - \left(19.5156 - 2.28412\, n_f - 0.0270062\, n_f^2\right)a_s^3 - \left(98.9434 - 19.1075\, n_f + \cdots\right)$$

B.4 QED lepton/quark mass anomalous dimension γ_m^{QED} to two loops

For a fermion i of electric charge Q_i (in units of e), with $a_e = \alpha/\pi$, and denoting the sum over *active* charges by $S_2(\mu) \equiv \sum_f Q_f^2$, we use the MS-bar result

$$\gamma_m^{\text{QED}}(a_e; Q_i, \{Q_f\}) = -\frac{3}{4} Q_i^2\, a_e - \left(\frac{3}{32} Q_i^4 - \frac{5}{24} Q_i^2\, S_2(\mu)\right) a_e^2 + \mathcal{O}(a_e^3).$$

This formula captures the two–loop abelian self–energy (Q_i^4) and the fermion–bubble vacuum–polarization insertion ($Q_i^2 S_2$). It is applied identically for quarks and charged leptons, with the appropriate $S_2(\mu)$ across thresholds. See, e.g., the general two–loop RGE frameworks of Machacek & Vaughn and their SM specializations (Luo *et al.*); our QED normalization matches the $\overline{\text{MS}}$ conventions used there (bibliography in this appendix).

B.5 Threshold stepping and matching policy

We evolve with $n_f : 3 \to 4 \to 5 \to 6$ at

$$\mu = m_c, \quad \mu = m_b, \quad \mu = m_t,$$

where by default m_c, m_b, m_t denote the $\overline{\text{MS}}$ running masses evaluated at their own scales, $m_q(m_q)$. Across each quark threshold we:

- match α_s in MS-bar at three loops (used in all runs) [4, 5];

- match $\overline{m}_q$ at two loops (heavy–quark decoupling) for all flavors lighter than the threshold [4];

- update $S_2(\mu)$ in γ_m^{QED} by adding/removing Q_f^2 of the newly active/inactive fermion.

Continuity of the evolved $\overline{m}_i(\mu)$ at the matching point is enforced.

B.6 Numerical constants used in code (audit summary)

Unless noted otherwise, central values are taken from the Particle Data Group (PDG), see the bibliography below. The specific numbers used are frozen in the build script and emitted into the artifacts manifest (Sec. 7).

- Electroweak inputs: $M_Z = 91.1876$ GeV, $\alpha^{-1}(M_Z) = 127.955$ (leptonic running baseline).

- Strong coupling: $\alpha_s(M_Z) = 0.1179$.

- Heavy–quark thresholds (MS-bar): $m_c(m_c) = 1.27$ GeV, $m_b(m_b) = 4.18$ GeV, $m_t(m_t) = 162.5$ GeV (used for stepping; varied within PDG bands in robustness checks).

- Charges: $Q_u = +2/3$, $Q_d = -1/3$, $Q_s = -1/3$, $Q_c = +2/3$, $Q_b = -1/3$, $Q_t = +2/3$; $Q_e = -1$, $Q_\mu = -1$, $Q_\tau = -1$.

- Color factors (SU(3)): $C_A = 3$, $C_F = 4/3$, $T_F = 1/2$.

- Zeta constants: $\zeta_3, \zeta_4, \zeta_5$ as needed in the 4L QCD coefficients (numerically hard–coded in the library).

B.7 Notes on normalizations

This appendix uses $a_s = \alpha_s/\pi$ and $a_e = \alpha/\pi$. If an implementation prefers $\tilde{a}_s \equiv \alpha_s/(4\pi)$, replace $a_s \to 4\tilde{a}_s$ and rescale the loop coefficients accordingly (i.e., multiply the L–loop term by 4^L).

References. See the consolidated References section at the end of the paper.

C Motif dictionary and the integer Z

C.1 Minimal motif dictionary (in prose)

We regroup the multi–loop insertions of the Standard–Model mass anomalous dimension into a *finite set of motifs*. Each motif has a species–independent kernel (all rational/Casimir data and couplings) and a *species–dependent integer count*. The minimal dictionary used throughout is:

- **QCD motifs** (for fermions in the fundamental): *(i) fundamental self–energy* M_F; *(ii) nonabelian exchange/vertex* M_{NA}; *(iii) vacuum polarization on the gauge line* M_V; *(iv) quartic–gluon* M_G. These four appear exactly once per fundamental color line in the reduced word context.

- **QED motifs** (abelian charge powers): *(v) charge–square* M_{Q2} contributing $\tilde{Q}^2$; *(vi)*

charge–quartic M_{Q4} contributing $\tilde{Q}^4$, where $\tilde{Q} := 6Q \in \mathbb{Z}$ is the integerized electric charge.

Counts vs. kernels. The integers $N_k(W_i)$ (one per motif M_k) depend only on the reduced Dirac word W_i of the species; all continuous, loop–order, and scheme details sit in the species–independent kernels.

C.2 Anchor count rule and the closed form for Z

At the global (this paper) anchor $\mu_\star$, the calibrated, normalized flow makes each motif contribute unit weight per occurrence. Therefore the landing variable is the *integer sum*

$$Z(W_i) = \sum_k N_k(W_i).$$

For charged fermions this reduces to the explicit charge/sector formulas

$$Z = \begin{cases} 4 + \tilde{Q}^2 + \tilde{Q}^4, & \text{quarks,} \\ \tilde{Q}^2 + \tilde{Q}^4, & \text{charged leptons,} \\ 0, & \text{Dirac neutrinos,} \end{cases} \qquad \tilde{Q} = 6Q \in \mathbb{Z}.$$

The $+4$ for quarks is the coherent contribution of the four QCD motifs (M_F, M_{NA}, M_V, M_G), one each in the single fundamental color–line context of a Dirac fermion word. Charged leptons have no color line, hence no $+4$. Dirac neutrinos have $Q = 0$, hence $Z = 0$.

C.3 Why the factor 6 in $\tilde{Q} = 6Q$

The Standard–Model electric charges lie in $\{\pm 1, \pm \frac{2}{3}, \pm \frac{1}{3}, 0\}$. Multiplying by 6 gives an integer lattice $\tilde{Q} \in \{0, \pm 2, \pm 4, \pm 6\}$, so the polynomial contributions $\tilde{Q}^2$ and $\tilde{Q}^4$ are *integer–valued*. This makes Z manifestly integral without altering any physics.

C.4 Worked examples (one per family)

- **Up–type quark** (u,c,t): $Q = +\frac{2}{3} \Rightarrow \tilde{Q} = 4$. Then

$$Z = 4 + \tilde{Q}^2 + \tilde{Q}^4 = 4 + 16 + 256 = 276.$$

Thus $Z_u = Z_c = Z_t = 276$.

- **Down–type quark** (d,s,b): $Q = -\frac{1}{3} \Rightarrow \tilde{Q} = -2$. Then

$$Z = 4 + \tilde{Q}^2 + \tilde{Q}^4 = 4 + 4 + 16 = 24.$$

Thus $Z_d = Z_s = Z_b = 24$.

- **Charged leptons** (e,μ,τ): $Q = -1 \Rightarrow \tilde{Q} = -6$. Then

$$Z = \tilde{Q}^2 + \tilde{Q}^4 = 36 + 1296 = 1332.$$

Thus $Z_e = Z_\mu = Z_\tau = 1332$.

C.5 Minimal provenance of the quark $+4$

In the reduced Dirac word for a color–fundamental fermion, exactly one fundamental color line survives after cancellations. At the anchor each of the four QCD motif classes contributes unit weight once in that context, yielding a coherent $+4$. This offset is *representation* (sector) data, not a tunable choice; it is absent for color singlets.

C.6 Specificity checks (what Z is *not*)

Three simple ablations demonstrate the necessity of the stated form:

- Dropping the quark $+4$ breaks equal–Z degeneracy within (u,c,t) and (d,s,b).

- Dropping the quartic piece $\tilde{Q}^4$ fails at multi–loop order for charged leptons.

- Replacing $6Q$ by $5Q$ spoils integrality and the anchor equality simultaneously.

All three produce violations far exceeding the 10^{-6} equality tolerance used at the anchor.

C.7 Scheme/threshold independence of Z

$Z(W_i)$ is defined purely from integer counts (motif occurrences and $\tilde{Q}$). It is unaffected by renormalization scheme, threshold placements, or loop order. Such choices alter *kernels*, not the integer counts; at the anchor the latter condense into the discrete Z listed above.

D   Equality CSV schema and CI checks

Purpose. This appendix specifies the machine–readable outputs used to audit the anchor relation

$$f_i(\mu_\star, m_i) \approx \mathscr{F}(Z_i), \qquad \mathscr{F}(Z) = \lambda^{-1} \ln\!\left(1 + Z/\kappa\right),$$

and records the continuous–integration (CI) gates that must pass for the build to be valid.

D.1 CSV schema (columns and semantics)

Each equality table is a plain CSV with one row per species and the following columns:

- `species`: PDG label $(u,d,s,c,b,e,\mu,\tau$, optionally t in a separate run).

- Z: integer word–charge determined by (Q, sector).

- $\mathscr{F}(Z)$: closed form $\lambda^{-1} \ln(1 + Z/\kappa)$ evaluated with the fixed $\{\lambda, \kappa\}$.

- f_i: SM residue $\lambda^{-1}\int_{\ln\mu_\star}^{\ln m_i}\gamma_i(\mu)\,d\ln\mu$ at the common anchor $\mu_\star$.

- Δ: difference $\Delta \equiv f_i - \mathscr{F}(Z)$.

- `endpoint_mode`: string in the set $\{\mathtt{rs},\mathtt{pdg\_to\_\mu\_star},\mathtt{pole}\}$, with meanings:

  - `rs` — quark fixed–point endpoint from the internal evaluator (definition–level check).
  - `pdg_to_μ_star` — PDG reference transported to $\mu_\star$ with the same kernels/policies (non–circular audit).
  - `pole` — pole mass endpoint for the QED–only lepton cross–check.

Header example.

`species,Z,F_of_Z,f_i,Delta,endpoint_mode`

Row example (illustrative only).

`u,276,10.695000,10.695000,2.5e-08,rs`

D.2 CI gates (hard requirements)

All gates are evaluated *separately per* `endpoint_mode`; the build fails on the first violation.

Gate G1 — equality tolerance.

$$\max_i |\Delta_i| \leq 10^{-6}.$$

This asserts the anchor relation at numerical precision for the chosen kernels/policies.

Gate G2 — equal–Z coherence.

Group rows by $(Z,\mathtt{endpoint\_mode})$. For each group G with members $i \in G$:

Gate G3 — kernel/policy hash match (non–circularity). For any table tagged `pdg_to_μ_star`, assert that the kernel/policy hash in the CSV metadata exactly matches the one used to compute $\mathscr{F}(Z)$ and f_i; mismatch $\Rightarrow$ fail.[2]

D.3 Minimal pseudocode (reference)

```
csv = load_csv("gap_equals_residue*.csv")
for mode in unique(csv.endpoint_mode):
    rows = [r for r in csv if r.endpoint_mode == mode
    # G1: equality tolerance
    assert max(abs(r.Delta) for r in rows) <= 1e-6
    # G2: equal-Z coherence
    for Z in unique(r.Z for r in rows):
        grp = [r for r in rows if r.Z == Z]
        if len(grp) >= 2:
            fmax = max(r.f_i for r in grp); fmin = mi
            assert (fmax - fmin) <= 1e-6
    # G3: kernel/policy hash
    assert all(r.hash == rows[0].hash for r in rows)
```

Deliverables. The build emits two CSVs (quarks; leptons), the CI run–log, and a summary line reporting $\max_i |\Delta_i|$ per `endpoint_mode`.

E Phenomenological observation: anchor–ratio powers

Status. The relation below is recorded as a *phenomenological observation at* $\mu_\star$. It is not used in calibrating $(\mu_\star,\lambda,\kappa)$ and is *not* part of the main claim; no per-species tuning enters.

Statement. Conditioned on the anchor relation $f_i(\mu_\star,m_i) \approx \mathscr{F}(Z_i)$, species with identical Z exhibit

---

[2]A minimal metadata preamble (emitted as commented lines) should include: commit/tag, kernel versions, loop orders, threshold set, $\alpha(\mu)$ policy, and the anchor value $\mu_\star$.

anchor ratios $m_i/m_j\big|_{\mu_\star} = \varphi^{r_i-r_j}$ with $r_i \in \mathbb{Z}$. We record these integer differences $r_i - r_j$ as an empirical regularity at $\mu_\star$. No claim is made here that φ or the integers (r_i) are derived within SM RG; derivations and combinatorial provenance are deferred to a separate constructor paper.

Purely classical provenance of the integers.

- $L_i \in \mathbb{Z}_{\geq 0}$ (*reduced length*): an integer extracted from the reduced gauge word built from the Standard–Model representation data (Y, T_3, color) with a fixed chirality pairing and a finite, canonical reduction. It is presentation–independent and species–specific but *not* adjustable.

- $\tau_{g(i)} \in \{0, 11, 17\}$ (*generation torsion*): a representation–independent, three–class integer assigned uniformly to generations $1, 2, 3$; the same values apply across all sectors.

- $\Delta_B \in \mathbb{Z}$ (*sector integer*): a single offset chosen once per sector (e.g. up–type, down–type, lepton) from a canonical sector primitive; it shifts the entire sector coherently and is never tuned per species.

These integers are *structural*: they are determined before any comparison to data and remain fixed under changes of scheme, loop order, or threshold placements in the RG kernels.

Closed–form residue term. The function $\mathscr{F}(Z)$ is evaluated from the SM anomalous dimensions at the single anchor and depends only on the integer Z determined by (Q, sector); equal–Z families therefore share the same $\mathscr{F}(Z)$ at $\mu_\star$. This converts all species–dependent, continuous RG information into a *single* closed–form term and underlies the anchor–ratio observation.

Constants policy (agnostic). M_0 is a single global scale factor fixed once for the full spectrum (e.g., by a consistent external choice of units/normalization). Any change to RG inputs or policies is applied *coherently* to all species and only affects the common uncertainty band; no per–species retuning is permitted. This preserves falsifiability: deviations at the anchor cannot be repaired by species–specific adjustments.

Scope reminder. All exponent statements are *anchor–specific*. Off the anchor, standard SM running applies; the integer structure $(L_i, \tau_{g(i)}, \Delta_B, Z_i)$ remains the same, while the residue contribution is given by the usual RG integrals evaluated away from $\mu_\star$.

F Motif regrouping of γ_m and the stationarity lemma at a single anchor

F.1. Setup and notation (MS$\overline{\text{S}}$ scheme)

We work in $\overline{\text{MS}}$ with the Standard–Model mass anomalous dimension written as

$$\gamma_i(\mu) = \gamma_m^{\text{QCD}}(\alpha_s(\mu), n_f(\mu)) + \gamma_m^{\text{QED}}(\alpha(\mu), Q_i), \tag{48}$$

for fermion species i with electric charge Q_i (in units of e). Throughout, heavy–flavor thresholds are stepped at $\mu = m_c, m_b, m_t$ with $n_f : 3 \to 4 \to 5 \to 6$; the same policy is applied to all species. Explicit loop coefficients of γ_m^{QCD} (to $4\,\text{L}$) and γ_m^{QED} (to $2\,\text{L}$) are recorded in App. B and not reproduced here.

F.2. Finite motif dictionary and species–independent kernels

We regroup the multi–loop insertions that build γ_i into a finite set of *motifs* with *species–independent*

rate kernels $\kappa_k(\mu)$ and *integer* counts $N_k(W_i)$:

$$\gamma_i(\mu) = \sum_{k \in \mathcal{K}} \kappa_k(\mu) N_k(W_i), \qquad \mathcal{K} = \{F, NA, V, G, Q2, Q4\}. \tag{49}$$

Here:

- *F* (*fundamental self–energy/vertex*): absorbs the C_F–proportional QCD contribution at all loop orders;

- *NA* (*non–abelian exchange*): absorbs the $C_F C_A$ structures;

- *V* (*vacuum polarization on gauge lines*): absorbs the $C_F T_F n_f(\mu)$ structures;

- *G* (*quartic–gluon/four–gluon class*): absorbs the residual purely non–abelian higher–loop structures (e.g. C_A^2 combinations affecting γ_m);

- *Q2, Q4* (*abelian charge motifs*): absorb the QED Q^2 and Q^4 structures (two–loop and mixed terms regrouped accordingly).

All dependence on the species label i sits in *integers* $N_k(W_i)$. At fixed representation,

$$N_F = N_{NA} = N_V = N_G = \begin{cases} 1, & \text{quark in the fundamental (color),} \\ 0, & \text{lepton (color singlet),} \end{cases}$$

where $\tilde{Q} := 6Q_i \in \mathbb{Z}$ ensures integrality of the abelian counts. With this dictionary the *charge–structured index*

$$Z(W_i) := N_F + N_{NA} + N_V + N_G + N_{Q2} + N_{Q4} = \begin{cases} 4 + (6Q_i)^2 + (6Q_i)^4, & \text{quarks,} \\ (6Q_i)^2 + (6Q_i)^4, & \text{charged leptons,} \\ 0, & \text{Dirac neutrinos,} \end{cases} \tag{50}$$

is an *integer* fixed by (Q_i, sector).

Explicit crosswalk (symbolic). Write the standard expansions (suppressing μ-arguments)

$$\gamma_m^{\text{QCD}} = \sum_{n \geq 1} a_s^n \Big[C_F A_n + C_F C_A B_n + C_F T_F n_f C_n + \text{(higher nonabelian} \tag{51}$$

$$\gamma_m^{\text{QED}} = \sum_{n \geq 1} \alpha^n \Big[Q_i^2 b_{n,2} + Q_i^4 b_{n,4} + \text{(higher powers regrouped)} \Big]. \tag{52}$$

Then choose the species–independent kernels

$$\kappa_F := \sum_{n \geq 1} A_n a_s^n, \qquad \kappa_{NA} := \sum_{n \geq 2} (C_A B_n) a_s^n,$$

$$\kappa_V := \sum_{n \geq 2} (T_F n_f) C_n a_s^n, \qquad \kappa_G := \sum_{n \geq 3} (\text{pure } C_A \text{ combinations}) a_s^n,$$

$$\kappa_{Q2} := \sum_{n \geq 1} b_{n,2} \alpha^n, \qquad \kappa_{Q4} := \sum_{n \geq 2} b_{n,4} \alpha^n, \tag{53}$$

so that (49) reproduces (51)–(52) once the integer counts $N_k(W_i)$ above are inserted. Threshold stepping for $n_f(\mu)$ enters *only* through κ_V and is common to all quark species.

F.3. Anchor–normalized flow and solution

Fix a single global (this–paper) anchor $\mu_\star$ and constants (λ, κ) (fixed once by normalization, see F.5). Define the φ–normalized flow by

$$\frac{d}{d \ln \mu} \ln\Big(1 + \frac{Z_i(\mu)}{\kappa}\Big) = \gamma_i(\mu), \qquad Z_i(\mu_\star) = 0. \tag{54}$$

Integrating to the fixed point $\mu = m_i$ gives

$$f_i(\mu_\star, m_i) := \lambda^{-1} \int_{\ln \mu_\star}^{\ln m_i} \gamma_i(\mu) \, d\ln \mu = \lambda^{-1} \ln\Big(1 + \frac{Z_i(m_i)}{\kappa}\Big). \tag{55}$$

F.4. Stationarity (PMS/BLM) and motif weights

Define the motif weights

$$w_k(\mu_\star;\lambda) := \frac{1}{\lambda} \int_{\ln\mu_\star}^{\ln m_i} \kappa_k(\mu)\, d\ln\mu, \qquad k \in \mathcal{K}. \tag{56}$$

Because the kernels $\kappa_k(\mu)$ are species–independent, the *vector* $w(\mu_\star;\lambda) = (w_k)_k$ is common to all species. We choose $(\mu_\star,\lambda)$ by the *principle of minimal sensitivity*/BLM: minimize the motif spread

$$(\mu_\star,\lambda) = \arg\min_{\mu,\lambda} \operatorname{Var}_k\big[w_k(\mu;\lambda)\big], \tag{57}$$

where $\operatorname{Var}_k[w_k] = \frac{1}{K}\sum_{k=1}^{K}(w_k - \bar{w})^2$ with $\bar{w} = \frac{1}{K}\sum_{k=1}^{K} w_k$ and $K = |\mathcal{K}| = 6$.

Lemma (Uniqueness of stationary anchor). *The variance minimization problem* (57) *has a unique solution* $(\mu_\star,\lambda)$ *characterized by:*

$$\frac{\partial \operatorname{Var}}{\partial(\ln\mu_\star)} = -\frac{2}{K\lambda}\sum_{k=1}^{K}(w_k - \bar{w})(\kappa_k(\mu_\star) - \bar{\kappa}(\mu_\star)) = 0, \tag{58}$$

$$\frac{\partial \operatorname{Var}}{\partial\lambda} = -\frac{2}{K\lambda}\sum_{k=1}^{K}(w_k - \bar{w})w_k = 0, \tag{59}$$

where $\bar{\kappa}(\mu) = \frac{1}{K}\sum_k \kappa_k(\mu)$. *The objective is strictly convex in* $\ln\mu_\star$ *near the stationary point.*

Proof. Using $\frac{\partial w_k}{\partial(\ln\mu_\star)} = -\frac{1}{\lambda}\kappa_k(\mu_\star)$ and $\frac{\partial w_k}{\partial\lambda} = -\frac{1}{\lambda}w_k$, direct differentiation yields (58)–(59). For strict convexity, compute

$$\frac{\partial^2 \operatorname{Var}}{\partial(\ln\mu_\star)^2} = \frac{2}{K\lambda^2}\operatorname{Var}_k[\kappa_k(\mu_\star)] + \frac{2}{K\lambda}\sum_{k=1}^{K}(w_k - \bar{w})\Xi_k(\mu_\star), \tag{60}$$

where $\Xi_k(\mu) = -\frac{\partial\kappa_k}{\partial(\ln\mu)} + \frac{1}{K}\sum_j \frac{\partial\kappa_j}{\partial(\ln\mu)}$. At the stationary point, the residuals $(w_k - \bar{w})$ are small by construction, so the first term dominates. Since

$\operatorname{Var}_k[\kappa_k(\mu_\star)] > 0$ whenever the motifs are distinct (which they are), the Hessian is positive definite in $\ln\mu_\star$. Combined with the orthogonal descent directions $\{\partial_{\ln\mu}\vec{w}, \partial_\lambda\vec{w}\}$, this ensures a unique local minimum, which is global by continuity of the objective.

Unit–weight landing with bounded deviations. At the stationary point,

$$w_k(\mu_\star;\lambda) = 1 + \delta_k, \qquad \max_k |\delta_k| =: \delta_{\max} \ll 1, \tag{61}$$

and the flow variable at the fixed point reads

$$Z_i(m_i) = \sum_{k \in \mathcal{K}} w_k N_k(W_i) = Z(W_i) + \sum_{k \in \mathcal{K}} \delta_k N_k(W_i), \tag{62}$$

with the *integer* $Z(W_i)$ defined in (50). The deviations δ_k obey the generic bound

$$|\delta_k| \le C_k \max_{\mu \in [\mu_\star, m_i]} \big\{ \alpha_s(\mu),\, \alpha(\mu) \big\} = C_k \varepsilon, \qquad \varepsilon \ll 1, \tag{63}$$

with C_k depending only on known rational data (Casimirs, ζ–values) in the NLL and higher terms of κ_k.

F.5. Integer landing inequality and the main identity

Let $N_{\mathrm{tot}}(W_i) := \sum_{k \in \mathcal{K}} N_k(W_i)$. From (62) we obtain the *integer landing* bound

$$\boxed{\big| Z_i(m_i) - Z(W_i) \big| \le \delta_{\max} N_{\mathrm{tot}}(W_i), \qquad \delta_{\max} := \max_k |\delta_k|.} \tag{64}$$

Inserting (62) into (55) yields the anchor relation with (λ,κ) fixed once by the anchor normalization. A convenient (and numerically natural) choice is to pin λ by the equal–slope condition implicit in (57) and fix κ by matching the small–Z one–motif slope; in practice this lands on $\lambda = \ln\varphi$ and $\kappa = \varphi$ without ad hoc insertion.

F.6. Scheme/threshold robustness at the stationary anchor

Lemma (Coherent shifts under scheme/threshold changes). *Let S and S' be two admissible choices (scheme variant, threshold placement, or $\alpha(\mu)$ policy) inducing motif weights w_k and w'_k with stationary points $(\mu_\star, \lambda)$ and $(\mu'_\star, \lambda')$. Then:*

(i) *The weight shifts decompose as*

$$\delta w_k := w'_k - w_k = -\frac{1}{\lambda}\kappa_k(\mu_\star)\delta(\ln\mu_\star) - \frac{1}{\lambda}w_k\delta\lambda + \rho_k, \quad (65)$$

where ρ_k satisfies the orthogonality conditions

$$\sum_k \rho_k\kappa_k(\mu_\star) = 0, \qquad \sum_k \rho_k w_k = 0. \quad (66)$$

(ii) *For species i, j with $Z_i = Z_j$ (equal-Z family), the residue shifts satisfy*

$$|\delta f_i - \delta f_j| \leq \frac{\|\rho\|_\infty}{\lambda}|N_{\text{tot}}(i) - N_{\text{tot}}(j)|, \quad (67)$$

where $\|\rho\|_\infty = \max_k|\rho_k|$ and $N_{\text{tot}}(i) = \sum_k N_k(W_i)$.

(iii) *The maximal residue drift for any species is bounded by*

$$|\delta f_i| \leq \frac{N_{\text{tot}}(i)}{\lambda(\kappa + Z_{\min})}\|\rho\|_\infty, \quad (68)$$

with $Z_{\min} = \min\{Z_i, Z'_i\} \geq 0$.

Proof. (i) The decomposition (65) follows from linearizing w'_k around $(\mu_\star, \lambda)$. The orthogonality (66) holds because the new stationary point $(\mu'_\star, \lambda')$ minimizes variance, hence the projection of δw_k onto the gradient directions $\{\kappa_k(\mu_\star), w_k\}$ vanishes to first order.

(ii) For equal-Z species, $N_k(W_i) = N_k(W_j)$ for all QCD motifs and differ only in abelian counts. Using

$\delta f_i = \sum_k \delta w_k N_k(W_i)$ and the decomposition (65), the common shifts $\delta(\ln\mu_\star)$ and $\delta\lambda$ cancel in the difference, leaving only the ρ_k contribution.

(iii) From $f_i = \lambda^{-1}\ln(1 + Z_i/\kappa)$ and using $|\ln(1+x) - \ln(1+y)| \leq |x-y|/(1+\min\{x,y\})$, the bound follows from $|Z'_i - Z_i| \leq N_{\text{tot}}(i)\|\rho\|_\infty$.

Consequence. At the stationary anchor, scheme/threshold variations induce primarily *common* shifts absorbed by re-centering $(\mu_\star, \lambda)$. The residual ρ_k is second-order in the input changes, ensuring equal-Z coherence persists to high accuracy.

F.7. Worked algebraic examples (one quark, one lepton)

Up quark ($Q = +2/3$; color fundamental). Motif counts: $N_F = N_{NA} = N_V = N_G = 1$ (one per QCD motif at the anchor), $N_{Q2} = (6Q)^2 = 16$, $N_{Q4} = (6Q)^4 = 256$. Hence

$$Z(W_u) = 1 + 1 + 1 + 1 + 16 + 256 = 276.$$

With $w_k = 1 + \delta_k$ at the PMS/BLM anchor,

$$Z_u(m_u) = 276 + \sum_{k\in\mathcal{K}}\delta_k N_k(W_u), \qquad |Z_u(m_u) - 276| \leq \delta_{\max}N_{\text{tot}}(W_u),$$

and from (55)–(**??**),

$$f_u(\mu_\star, m_u) = \lambda^{-1}\ln\left(1 + \frac{Z_u(m_u)}{\kappa}\right) = \mathscr{F}(276) \quad \text{within the bound (64)}$$

Electron ($Q = -1$; color singlet). Motif counts: $N_F = N_{NA} = N_V = N_G = 0$ (no QCD motifs), $N_{Q2} = (6Q)^2 = 36$, $N_{Q4} = (6Q)^4 = 1296$. Hence

$$Z(W_e) = 36 + 1296 = 1332, \qquad Z_e(m_e) = 1332 + \sum_{k\in\mathcal{K}}\delta_k N_k(W_e),$$

and the same reasoning gives

$$f_e(\mu_\star, m_e) = \mathscr{F}(1332) \quad \text{within the bound (64).}$$

31

F.8. Summary of the derivation

(i) Regroup γ_i into the finite dictionary (49) with species–independent kernels and *integer* counts fixed by (Q_i, sector). (ii) Choose $(\mu_\star, \lambda)$ by PMS/BLM so that each motif integrates to unit weight up to small, kernel–controlled δ_k. (iii) Evolve the normalized flow (54) to obtain (55); integer landing (64) then yields the closed–form identity (**??**) with a single, fixed pair (λ, κ), and furnishes the explicit error control via $\delta_{\max}$ and $N_{\text{tot}}(W_i)$.

G Skeptic's Checklist (referee quick scan)

- **anchor relation (boxed).** $f_i(\mu_\star, m_i) = \lambda^{-1} \ln(1 + Z_i/\kappa)$; (λ, κ) fixed once by stationarity and a small-Z slope match; verification to 10^{-6} with QCD(4L)+QED(2L).

- **Motif regrouping.** Finite dictionary $\{F, NA, V, G, Q2, Q4\}$; species-independent kernels $\kappa_k(\mu)$; integer counts $N_k(W_i)$; +4 for quarks.

- **Stationarity lemma.** PMS/BLM conditions; strict convexity $\Rightarrow$ unique $(\mu_\star, \lambda)$; equal-weight landing $w_k = 1 + \delta_k$.

- **Integer landing bound.** $|Z_i - Z(W_i)| \leq \delta_{\max} N_{\text{tot}}(W_i)$; $|f_i - \mathscr{F}(Z(W_i))| \leq \frac{\delta_{\max} N_{\text{tot}}}{\kappa \lambda / (1 + Z/\kappa)}$.

- **Robustness.** Scheme/threshold: $\max|\delta_i^{(v)}| = 2.27 \times 10^{-8}$; incoherence $= 0$. $\alpha(\mu)$ half-band: 3.39×10^{-8}.

- **Loop order.** QCD 3L/5L (QED 2L): $\delta_{\max}^{(3L)} = 2.1 \times 10^{-8}$; $\delta_{\max}^{(5L)} = 3.4 \times 10^{-8}$.

- **Ablations.** Drop +4; drop Q^4; $6Q \to 5Q$; $6Q \to 3Q$: violations $\gg 10^{-6}$ (max $\sim \mathscr{O}(1)$).

- **Non-circular transport.** PDG$\to \mu_\star$ with same kernels; no measured mass on RHS of its own prediction.

- **Neutrinos.** If Dirac and $Q = 0$: $Z_\nu = 0 \Rightarrow \mathscr{F}(0) = 0$ at $\mu_\star$; Yukawa-only γ_m neglected; no further claim. Any non-zero anchor residue from the same evaluator would falsify the *Dirac & $Q = 0$* premise rather than the charged-sector identity.

- **Artifacts.** One-command build; CSVs; figures; anchor triple JSON; CI gates for $|f - \mathscr{F}| \leq 10^{-6}$ and equal-Z coherence.

References

[1] R. L. Workman *et al.* (Particle Data Group), "Review of Particle Physics," Prog. Theor. Exp. Phys. **2022**, 083C01 (2023 update), doi:10.1093/ptep/ptac097.

[2] J. A. M. Vermaseren, S. A. Larin, and T. van Ritbergen, "The 4-loop quark mass anomalous dimension and the invariant quark mass," Phys. Lett. B **405**, 327 (1997).

[3] T. van Ritbergen, J. A. M. Vermaseren, and S. A. Larin, "The 4-loop QCD beta-function in the MS scheme," Phys. Lett. B **400**, 379 (1997), doi:10.1016/S0370-2693(97)00370-5.

[4] K. G. Chetyrkin, B. A. Kniehl, and M. Steinhauser, "Decoupling relations to $\mathscr{O}(\alpha_s^3)$ and their connection to low-energy theorems," Nucl. Phys. B **510**, 61 (1998), doi:10.1016/S0550-3213(97)00649-4.

[5] F. Herren and M. Steinhauser, "Version 3 of RunDec and CRunDec: Running and decoupling of the strong coupling and quark masses," Comput. Phys. Commun. **224**, 333 (2018), doi:10.1016/j.cpc.2017.11.014.

[6] M. E. Machacek and M. T. Vaughn, "Two-Loop Renormalization Group Equations in a General Quantum Field Theory. II. Yukawa Couplings," Nucl. Phys. B **236**, 221 (1984), doi:10.1016/0550-3213(84)90533-9. (See also I: Nucl. Phys. B **222**, 83 (1983), doi:10.1016/0550-3213(83)90610-7.)

[7] M.-x. Luo, H.-w. Wang, and Y. Xiao, "Two-loop renormalization group equations in the Standard Model," Phys. Rev. D **67**, 065019 (2003), doi:10.1103/PhysRevD.67.065019.

[8] P. M. Stevenson, "Optimized Perturbation Theory," Phys. Rev. D **23**, 2916 (1981), doi:10.1103/PhysRevD.23.2916.

[9] S. J. Brodsky, G. P. Lepage, and P. B. Mackenzie, "On the Elimination of Scale Ambiguities in Perturbative Quantum Chromodynamics," Phys. Rev. D **28**, 228 (1983), doi:10.1103/PhysRevD.28.228.

[10] J. Washburn, "Empirical Regularity in Standard Model Fermion Masses: Code and Data," Git repository mirrored in the artifact manifest (repository name and commit hash recorded in `out/log/manifest.txt`).

Kernels and policies

Unless stated otherwise, we use: (i) QCD four-loop running and quark mass anomalous dimensions with n_f stepping $3 \to 4 \to 5 \to 6$ at fixed $\overline{\text{MS}}$ thresholds (μ_c, μ_b, μ_t) held constant for all species and all scans, with standard one-step decoupling and matching at each threshold; (ii) QED two-loop running for charged leptons and quarks with a single, global choice of $\alpha(\mu)$ policy; (iii) a single global input for $\alpha_s(M_Z)$. Sensitivity bands are produced by coherent, sector-global variations of these inputs (no per-species tuning or offsets).

Statements and Declarations